CMAT
Centro de Matemática

Universidade do Minho

Dynamic Neural Fields as a Mathematical Framework to model Cognitive Brain Functions

Wolfram Erlhagen
CMAT

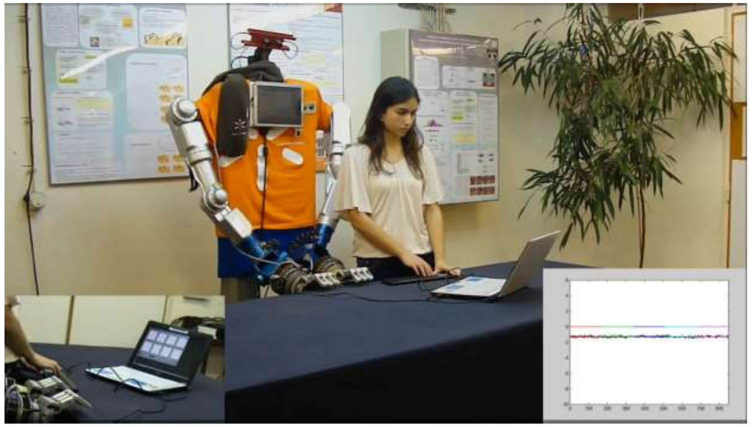

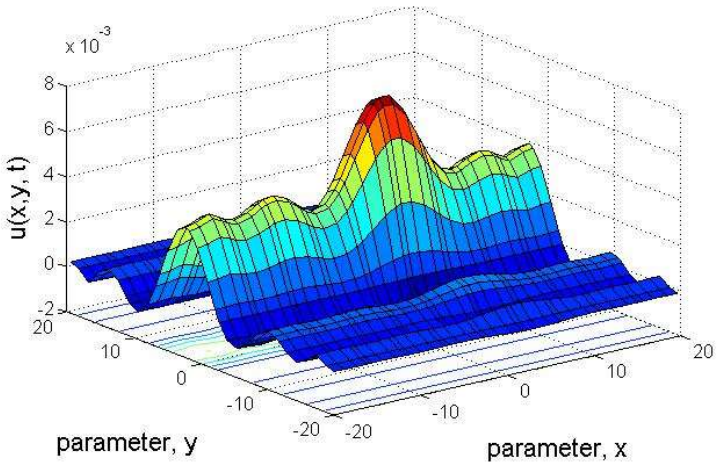

02.04.2023

7ª edição do Encontro Nacional de Estudantes de Matemática (ENEMath23), Porto

https://www.fc.up.pt/enemath/index.php

Mutidisicplinary Approach

Cognitive Science

reaction time, errors

Neuroscience

multi-electrode recordings
EEG, fMRI, ERN

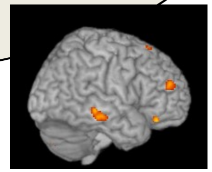

Mathematics & Modelling

Dynamic Field theory, optimization, statistics
machine learning etc.

$$\frac{\partial u(x,t)}{\partial t} = -u(x,t) + \int_{-\infty}^{+\infty} w(x-x')\; f(u(x',t))\; dx'$$

Cognitive Artifical Agents

artifical intelligence,
human-robot interactions (HRI),
intelligent driver assistant

Overview

Dynamic Neural Fields

1. Neurophysiological motivation

2. Mathematical analysis of pattern formation
   - single- and multi-bump solutions
   - new mathematical challenges

3. Application for the design of Cognitive Artifical Agents
   - case study: learning sequential tasks
     - human-robot interactions
     - intelligent diver assistant

4. Outlook

What is Mathematical Neuroscience?

Development and analysis of **mathematical models** that help to elucidate the fundamental mechanisms responsible for **experimentally observed behaviors** in neuroscience at **all relevant scales**, from the molecular world to that of cognition.

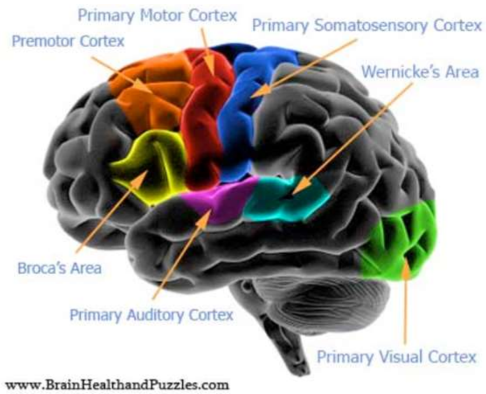

Levels of Description:
From Molecules to Neural Networks

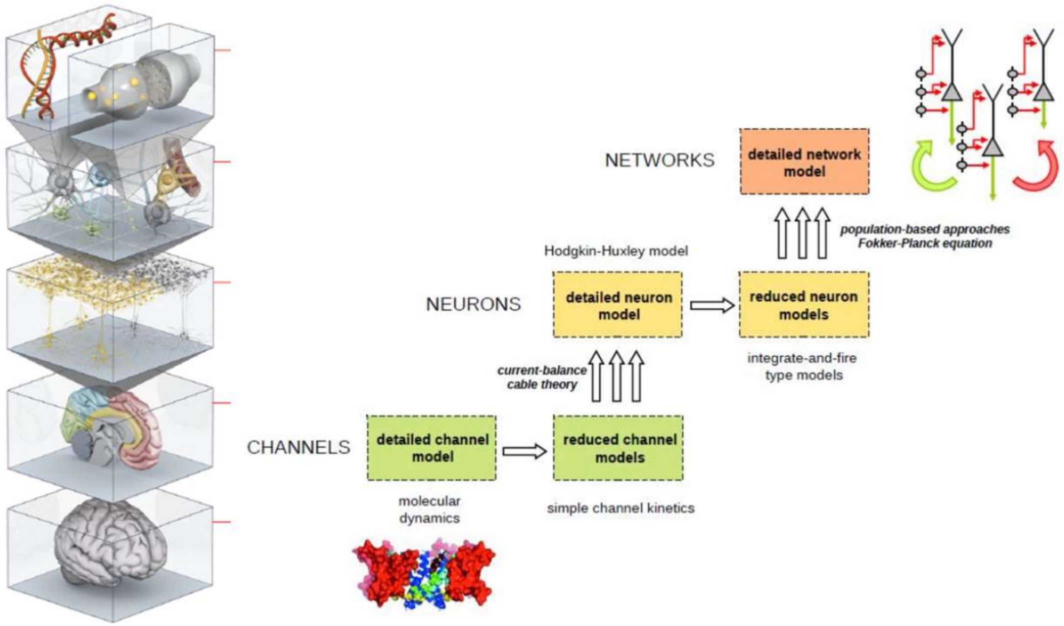

Neural Information Processing

Electrical signal: the change of voltage in the cell membrane of a neuron results in a voltage spike called an <u>Action Potential</u> which propagates along the axon.

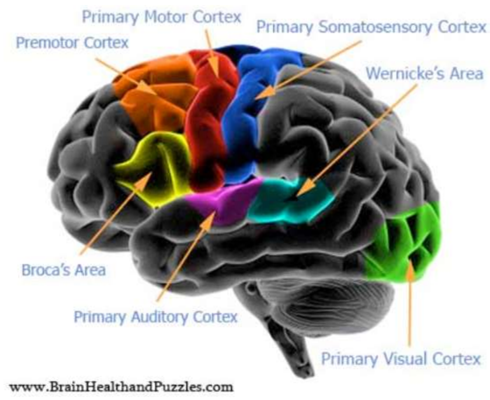

all-or-none principle

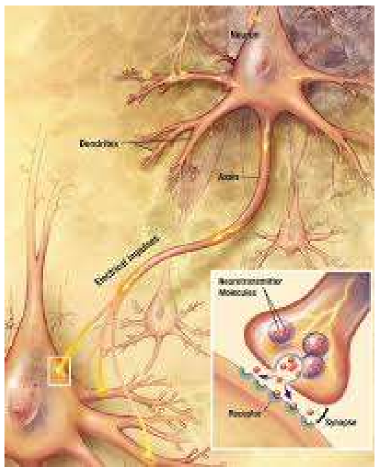

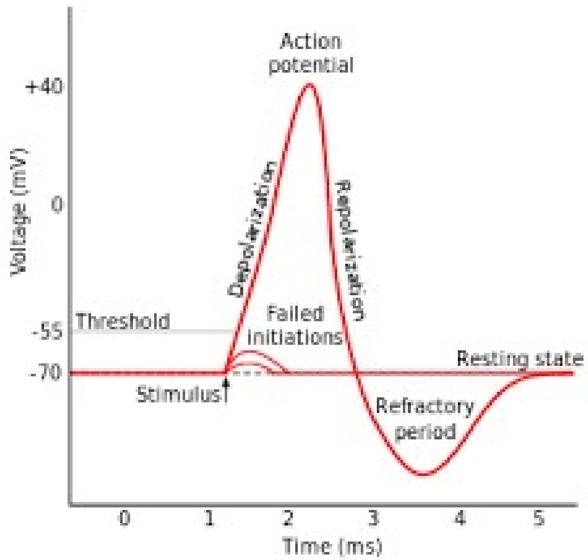

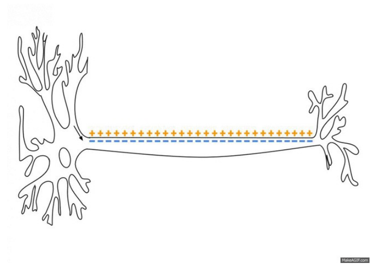

Neural Firing:
The Hodgkin-Huxely Model (1952)

The mathematical model consists of a system of 4 nonlinear ordinary differential equations:

$$I = C_m \frac{dV_m}{dt} + g_k n^4 (V_m - V_k) + g_{Na} m^3 h (V_m - V_{Na}) + g_l (V_m - V_l)$$

$$\frac{dn}{dt} = \alpha_n(V_m)(1-n) - \beta_n(V_m) n$$

$$\frac{dm}{dt} = \alpha_m(V_m)(1-m) - \beta_m(V_m) m$$

$$\frac{dh}{dt} = \alpha_h(V_m)(1-m) - \beta_h(V_m) h$$

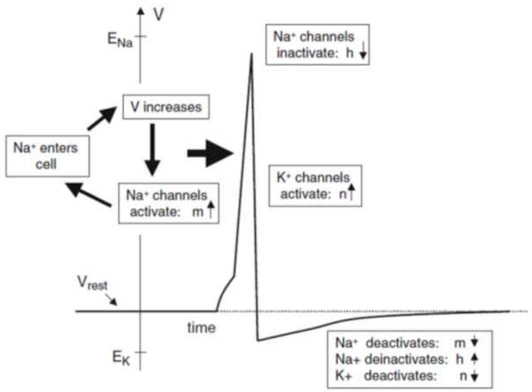

where I- current; V_m - membrane potential, n, m, h -quantities describing activation of sodium ion channel, activation of potassium ion channel and inactivation of sodium ion channel;α_i, β_i - constant rates; g_i-conductances.

FitzHugh–Nagumo model (1961)

Reduction to **two-dimensional model** for analytical treatment

- a brief stimulus $\boldsymbol{I}$ leads to nonlinear increase of membrane voltage $\boldsymbol{v}$, diminished over time by a slower, linear recovery variable $\boldsymbol{w}$

$$\frac{dv}{dt} = v - \frac{v^3}{3} - w + I$$

$$\frac{dw}{dt} = \frac{1}{\tau}(v + a - bw)$$

Phase plane analysis

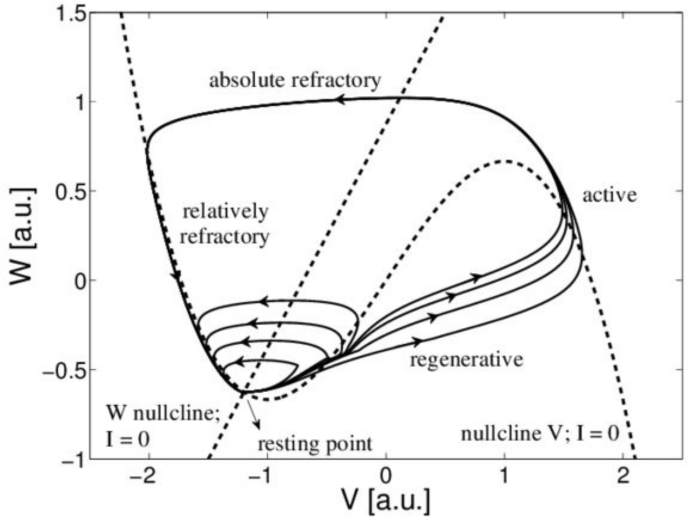

Spike train

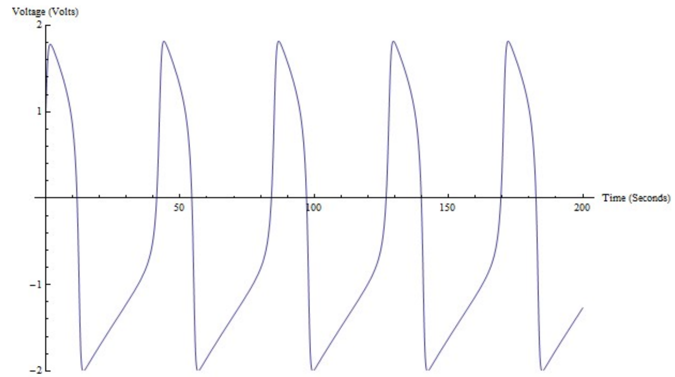

$a = 0.7, b = 0.8;\ \tau = 13, I = 0.5$

Impressive Numbers

<u>Human Brain</u>

$$\sim 10^{12}\ Neurons$$
$$\sim 10^{15}\ Synapses$$

$\Rightarrow 1mm^3$ of cortex ~ 1 billion connections

Computational Neuroscience

- Flagship European Blue Brain Project (http://bluebrain.epfl.ch/)
- US Brain Initiative (https://braininitiative.nih.gov/)

Using **supercomputers** to simulate all the cells and most of the synapses in an entire brain, thereby hoping to “challenge the foundations of our understanding of intelligence and generate new theories of consciousness.”

Neural Field Approach

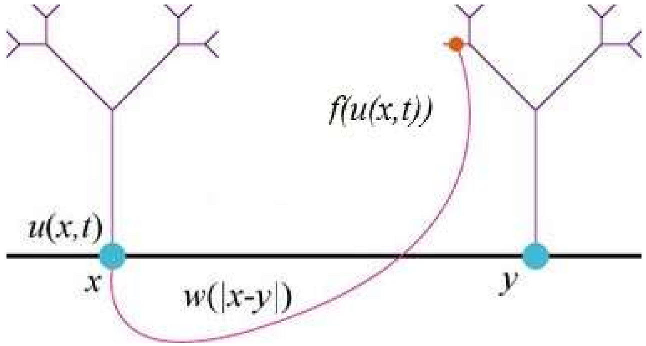

Neural field models consider:

- a **spatial continuum approximation** of the network**,** neural population activity described by a field $u(x,t)$ in terms of a time t and a spatial coordinate x;
- **population firing rates** measured in a certain short time interval of a few milliseconds;
- $f(u)$ firing rate function;
- $w(|x-y|)$ connection strength to a neuron separated by a distance y, system is assumed to be **spatially homogeneous and isotropic**.

Mathematical Formulation

- *Wilson & Cowan 1973*
  - separate exitatory and inhibitory populations
  - one-dimensional field, $x \in \mathbb{R}$

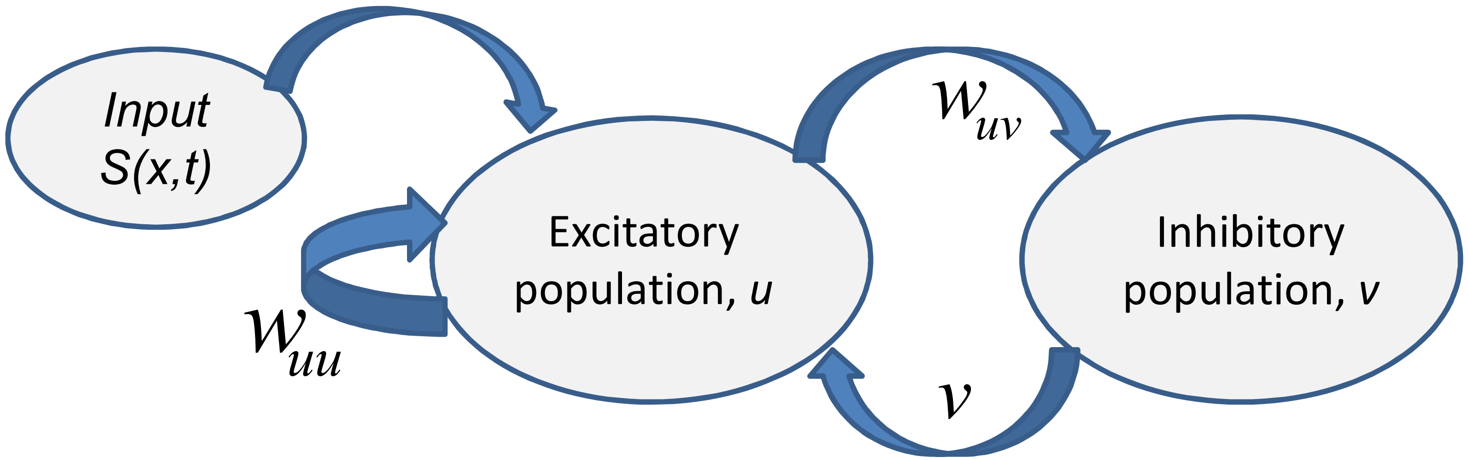

$$\frac{\partial u(x,t)}{\partial t} = -u(x,t) + \int_{-\infty}^{+\infty} w_{uu}(x-x')\ f(u(x',t))\,dx' - v(x,t) + S(x,t)$$

$$\frac{1}{\varepsilon}\frac{\partial v(x,t)}{\partial t} = -v(x,t) + \int_{-\infty}^{+\infty} w_{uv}(x-x')\ f(u(x',t))\,dx', \quad \varepsilon \in R$$

Amari’s Model of Lateral Inhibition

$\varepsilon \gg 1$: inhibition much faster than excitation (Amari 1977)

$$\frac{\partial u(x,t)}{\partial t} = -u(x,t) + \int_{-\infty}^{+\infty} w(x-x')\, f(u(x',t))\, dx' - h + S(x,t)$$

with $\quad w(x-x') = w_{uu}(x-x') - w_{uv}(x-x')$

- $u(x,t)$: activity at position $x \in \mathbb{R}$ and time t
- $w(x,x') = w(|x-x'|)$: distance-dependent
- $f(u)$: sigmoidal output function
- $h > 0$: global inhibition, defines resting state
- $S(x,t)$: time-dependent localized input

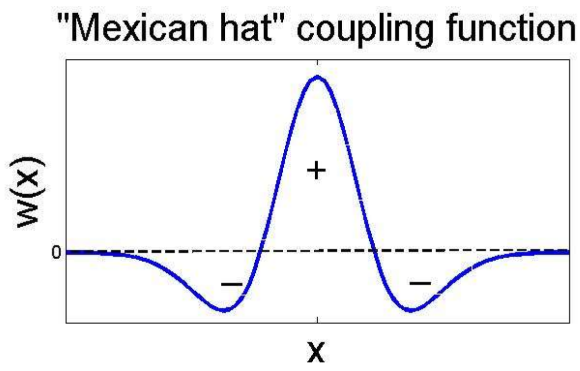

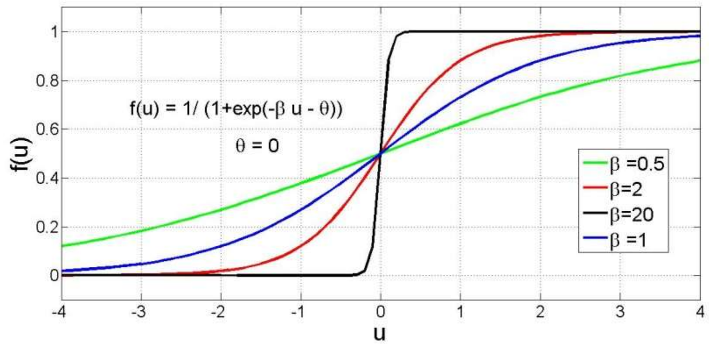

➢ **Possible generalization to the case $x \in \Omega \subseteq \mathbb{R}^n$**

Formation of different Patterns

- space-time plots of a one-dimensional fields

multi-bump

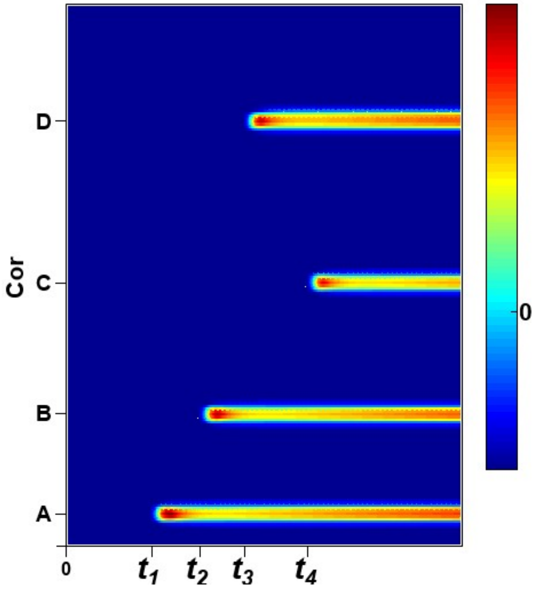

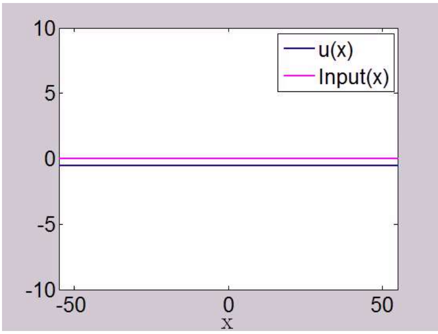

traveling bump

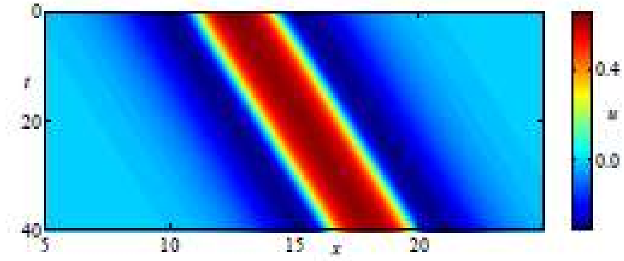

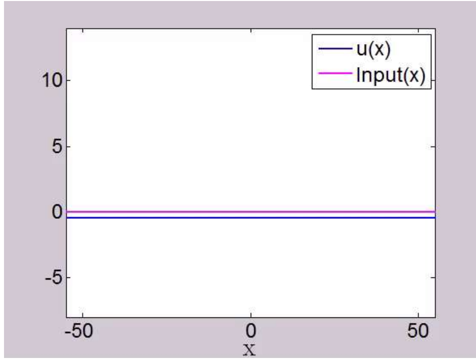

breather

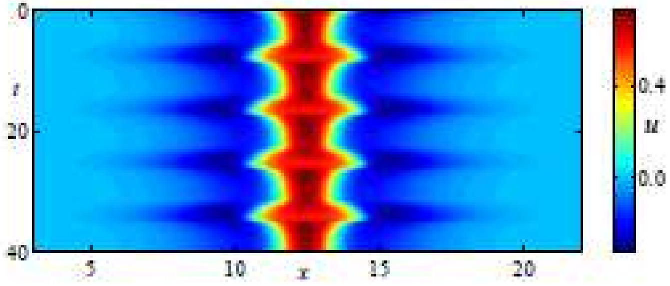

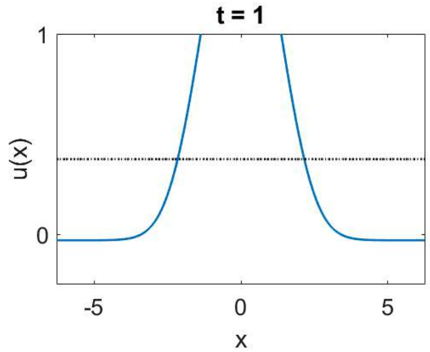

Basic Concepts of Dynamic Field Theory

- neural fields are spanned over continuous dimensions, e.g., movement direction, color, tone pitch …..
- self-stabilized, localized excitation patterns or bumps triggered by external input are the units of representation

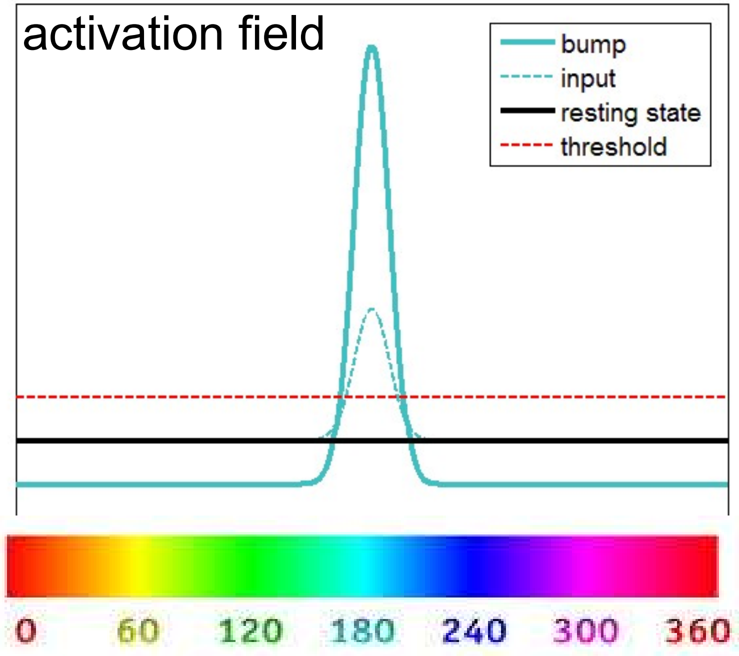

- operate in **bi-stable regime**: homogeneous resting state co-exists with bump attractor, transient input may switch between the two stable states

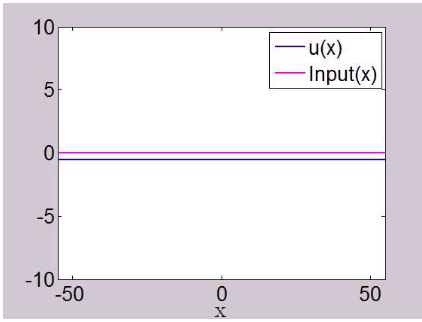

Field Dynamics: Cognitive Functions

transient external input S(x,t)

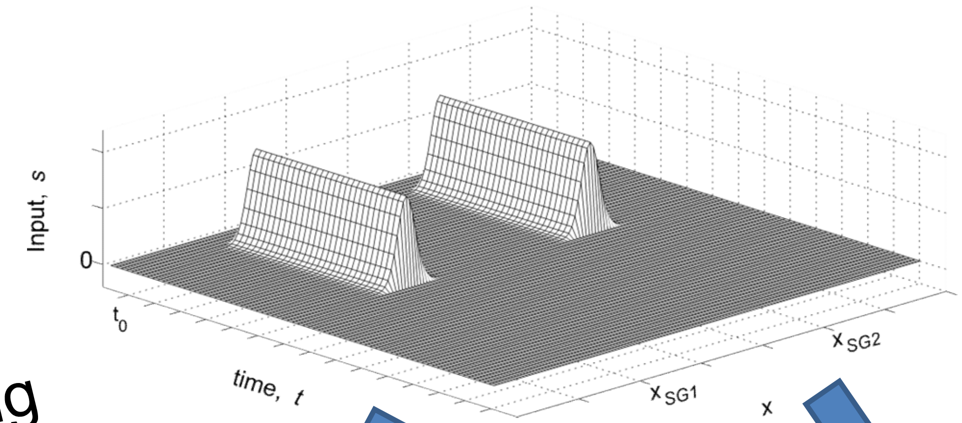

decision making

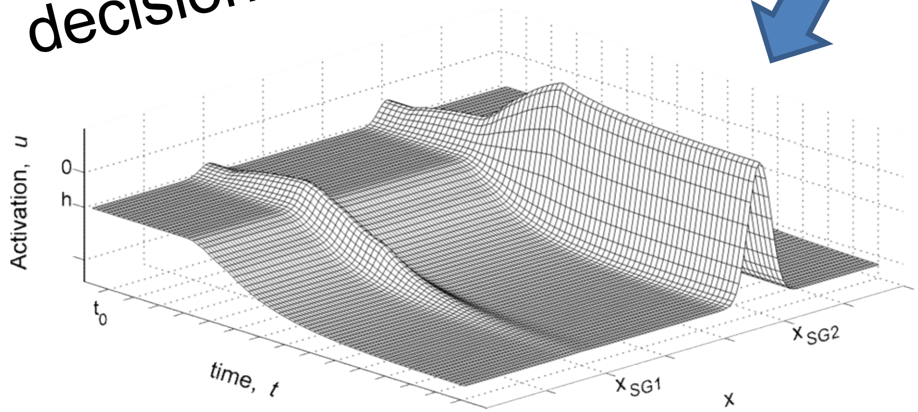

working memory

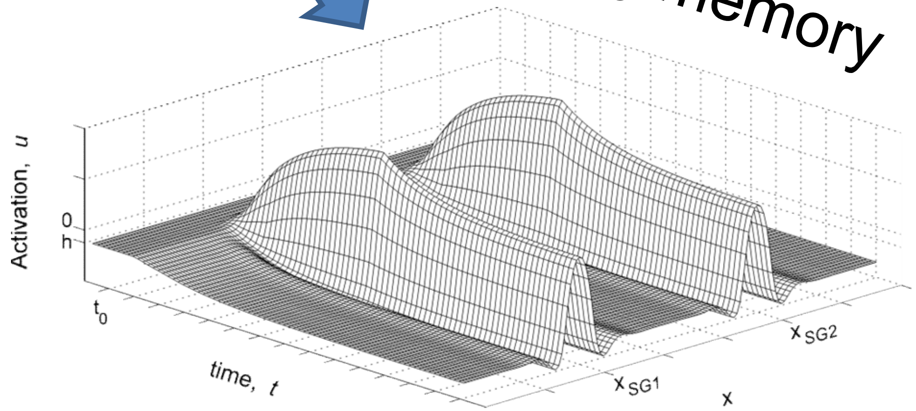

Neural evidence for localized activity patterns in parametric space

Example: Movement direction

Center-out task

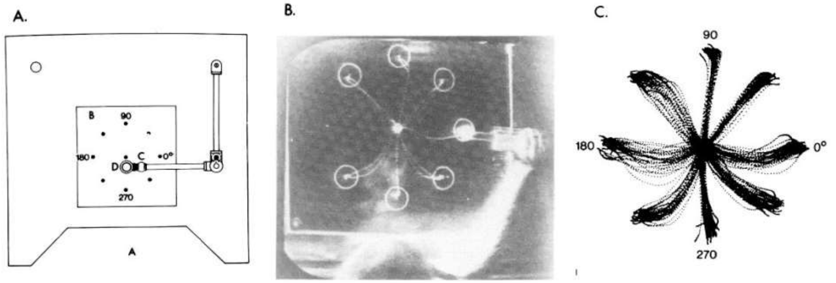

Neural tuning curve

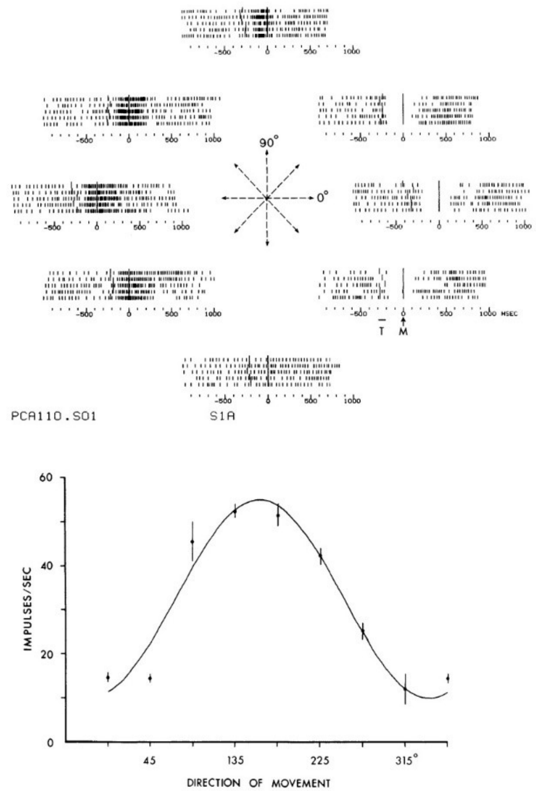

DPA method: Premotor cortex of monkey

Distributed Population Activation (DPA) technique:

$$u_k(x) = \sum_{neur\quad ,i} f_i^k \, b_i(x)$$

$f_i^k =$ neural firing rate of neuron i, in experimental condition k

$b_i(x) =$ basis function contributed by each neuron (e.g., normalized tuning curve)

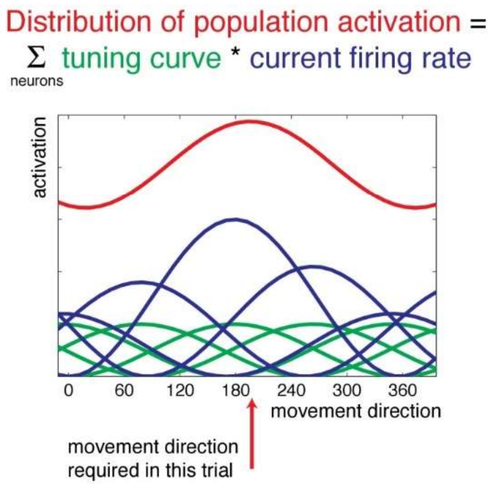

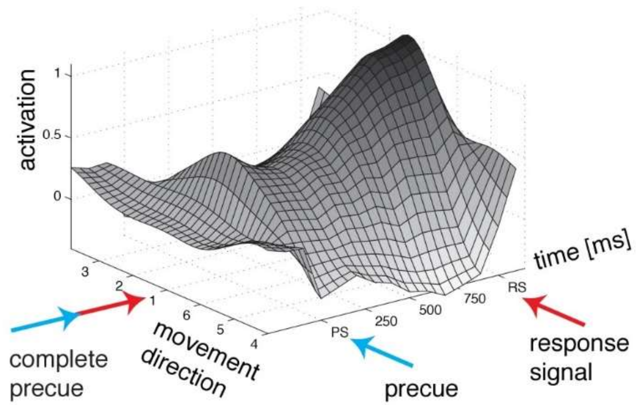

Bastian et al. *NeuroReport* (1998)
Erlhagen et al, *J. Neuro Methods*(1999)

Amari's analysis of bump solutions: Heaviside world

Stationary localized excitation pattern or **bump** (case S(x)=0):

$$\frac{\partial u(x,t)}{\partial t} = 0: \qquad u(x) = \int_{-\infty}^{+\infty} w(x-y) f(u(y,t)dy - h \qquad (1)$$

With the definition $R[u] = \{x: u(x) > 0\}$ and the choice of the Heaviside function

$$f(u) = H(u) = \begin{cases} 0, & u \leq 0 \\ 1, & u > 0 \end{cases}$$

it follows

$$u(x) = \int_{R[u]}^{\cdot} w(x-y)dy - h \qquad (2)$$

Mathematical Analysis: Heaviside World

A stationary bump of width a satisfies:

$$u(x) = \int_0^a w(x-y)dy - h = W(x) - W(x-a) - h \quad (3)$$

with $\quad W(x) = \int_0^x w(y)\, dy$

Since $u(0) = u(a) = 0$, a necessary condition for existence is

$$\boxed{W(a) = h}$$

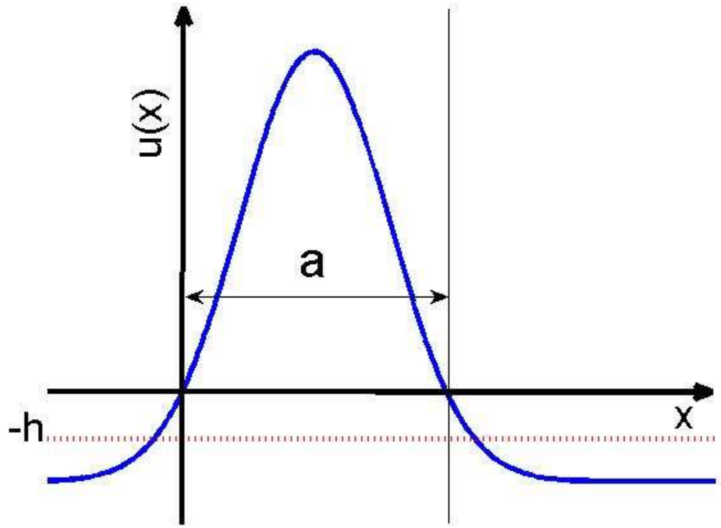

Existence of Bump Solutions

Two quantities to caracterize field properties:

$$W(x) = \int_0^x w(y)\,dy$$

$$W_{\max} = \max(W(x))$$

Theorem (Amari 1977)

If $W(\infty) < 0$ and $W_{\max} > h > 0$ hold, there exist two solutions a_1, a_2 with $a_2 > a_1$ together with the homogeneous solution $u(x) = -h$.

Coupling function $w(x)$ of lateral inhibition type

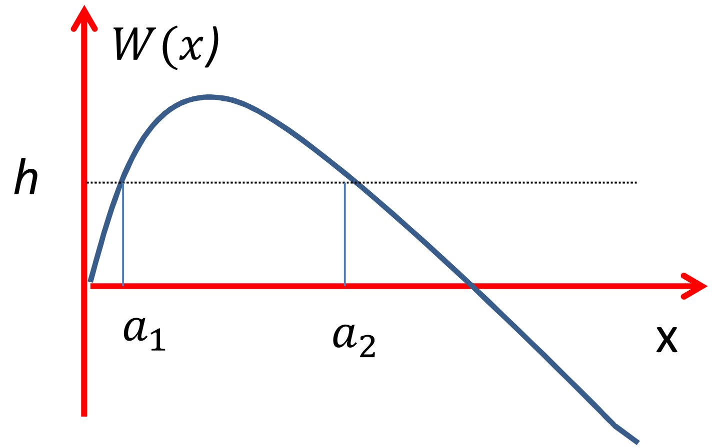

Stability of Bump Solutions

- consider a bump solution $u(x,t)$ not necessarely an equilibrium with the excited region at time t given by : $R[u(x,t)] = (x_1(t), x_2(t))$

at time t: $u(x_i,t) = 0$ at time $t + dt$: $u(x_i + dx_i, t + dt) = 0$

- track the motion of the boundary points by:

$$\frac{\partial u(x_i,t)}{\partial x} dx_i + \frac{\partial u(x_i,t)}{\partial t} dt = 0$$

- since $u(x_i,t) = 0$ at time t it follows:

$$\frac{\partial u(x_i,t)}{\partial t} = \int_{x_1(t)}^{x_2(t)} w(x-y)dy - h = W(x_2(t) - x_1(t)) - h$$

$$\frac{dx_1}{dt} = \frac{-\partial u}{\partial t} \Big/ \frac{\partial u}{\partial x} = -\frac{1}{c1}[W(x_2 - x_1) - h] \quad with\ \ c1 = \frac{\partial u(x_1,t)}{\partial x}$$

$$\frac{dx_2}{dt} = \frac{1}{c2}[W(x_2 - x_1) - h] \quad with\ \ c2 = -\frac{\partial u(x_2,t)}{\partial x}$$

Stability of Bump Solutions

The change of lenght of the excited region is governed by the equation

$$\frac{da(t)}{dt} = \left(\frac{1}{c1} + \frac{1}{c2}\right)\{W(a) - h\} \quad \text{with } a(t) = x_2(t) - x_1(t)$$

The equilibrium lenght is given by $W(a) - h = 0$

Bump is stable if and only if
$$w(a) = W'(a) < 0.$$

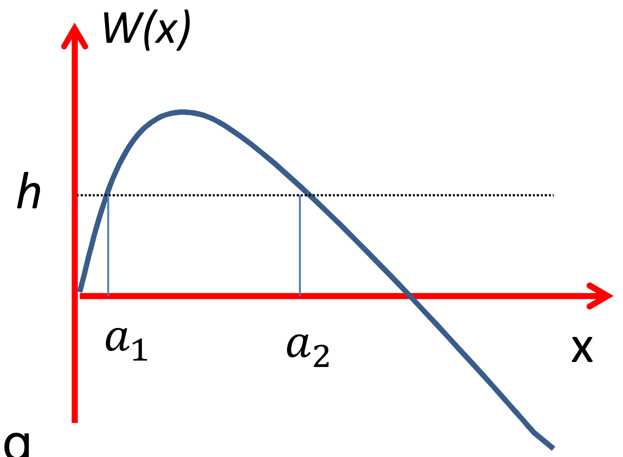

- Generalization to **sigmoid nonlinearity** using tools from **functional analysis**

Linear Stability Analysis

- perturbation of the stationary solution $U(x)$: $u(x,t) = U(x) + \Psi(x,t)$

$$\frac{\partial \Psi(x,t)}{\partial t} = -\Psi(x,t) + \int_{-\infty}^{\infty} w(|\mathrm{x}-y|) f'\big(U(y)\big)\Psi(y,t)dy$$

- assuming $\Psi(x,t) = e^{\lambda t}\big(\Psi(x)\big)$:

$$\lambda\Psi(x_1) = -\Psi(x_1) + \frac{w(0)\Psi(x_1)}{|U'(x_1)|} + \frac{w(a)\Psi(x_2)}{|U'(x_2)|}$$

$$\lambda\Psi(x_2) = -\Psi(x_2) + \frac{w(a)\Psi(x_1)}{|U'(x_1)|} + \frac{w(0)\Psi(x_2)}{|U'(x_2)|}$$

with c $= |U'(x_i| = w(0) - w(a)$, $i = 1{,}2$

- in matriz form: $A\begin{pmatrix}\Psi(x_1)\\ \Psi(x_2)\end{pmatrix} = \begin{pmatrix}0\\0\end{pmatrix}$ $\;with\;\; A = \begin{bmatrix}\lambda+1-a & -b\\ -b & -b\lambda+1-a\end{bmatrix}$

with a $= \frac{w(0)}{c}$, $b = \frac{w(a)}{c}$

- eigenvalues of A: $\boxed{\boldsymbol{\lambda_- = 0;\quad \lambda_+ = \frac{2\,w(a)}{w(0)-w(a)}}}$ $\boxed{\Rightarrow \mathrm{Re}(\lambda_+) < 0 \text{ if } w(a) < 0}$

Continuous Bump Attractor

- zero eigenvalue reflects translation invariance of the recurrent interactions

  $\Rightarrow$ bump marginally stable to perturbations in position

Bump searching for the maximum of $S(x)$

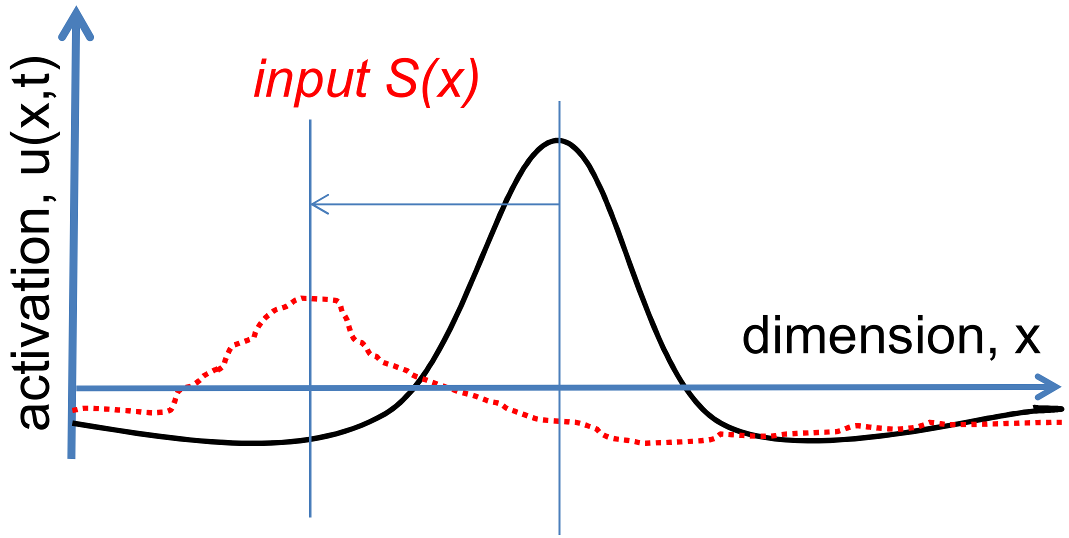

Robotics Application

- Detection and tracking of a moving object

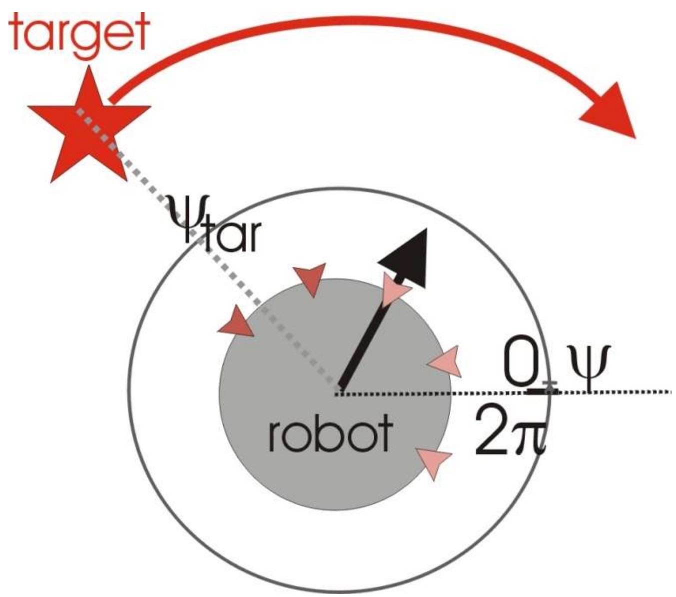

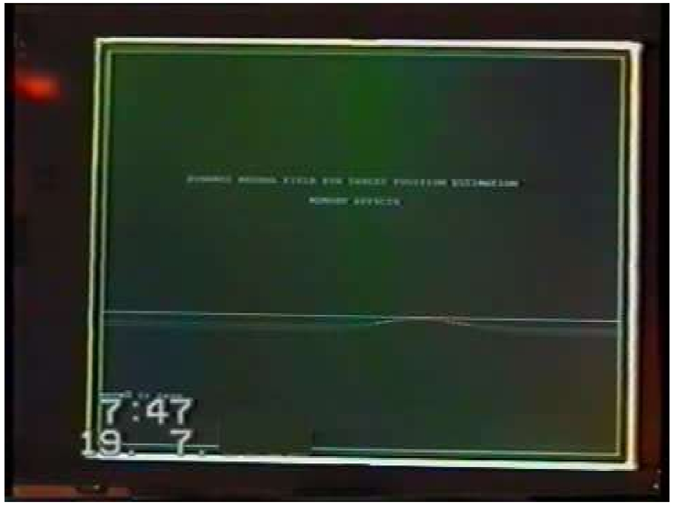

Bicho et al., *Int. J. Rob. Res*. (2000)

Computer Vision Application

- 2D tracking of multiple moving fish larvae

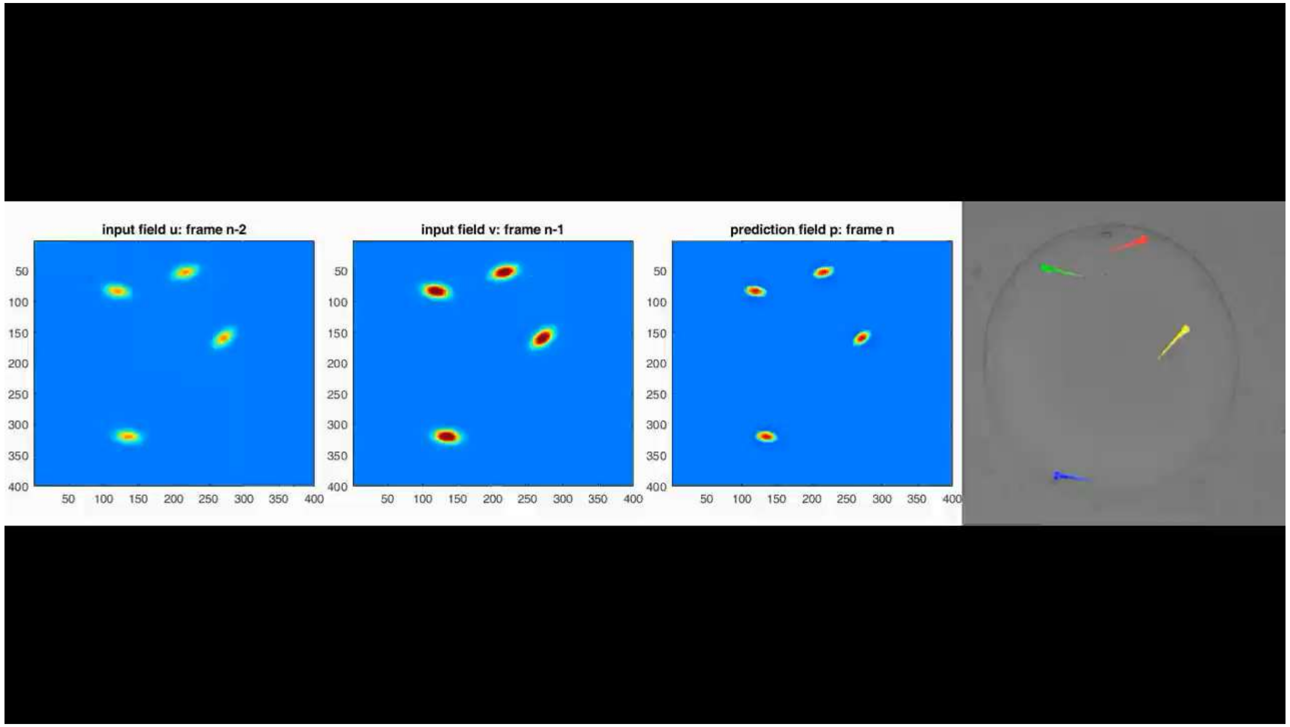

Kamkar at al, *Neural Networks (*2022)

Field Equation with Additive Noise: Diffusive Bump Drift

$$\frac{\partial u(x,t)}{\partial t} = -u(x,t) + \int_{-\infty}^{+\infty} w(|x-y|)\, f(u(y,t))dy - h + S(x,t) + \boldsymbol{\varepsilon^{1/2}\, dW(x,t)}$$

where $dW(x,t)$ is the increment of a spatially correlated Wiener process.

Neural evidence in monkey Prefrontal Cortex (PFC):

- Bump attractor dynamics in **PFC** explains **behavioral precision** in a working memory task.

Wimmer et al., *Nature Neuroscience* (2014)

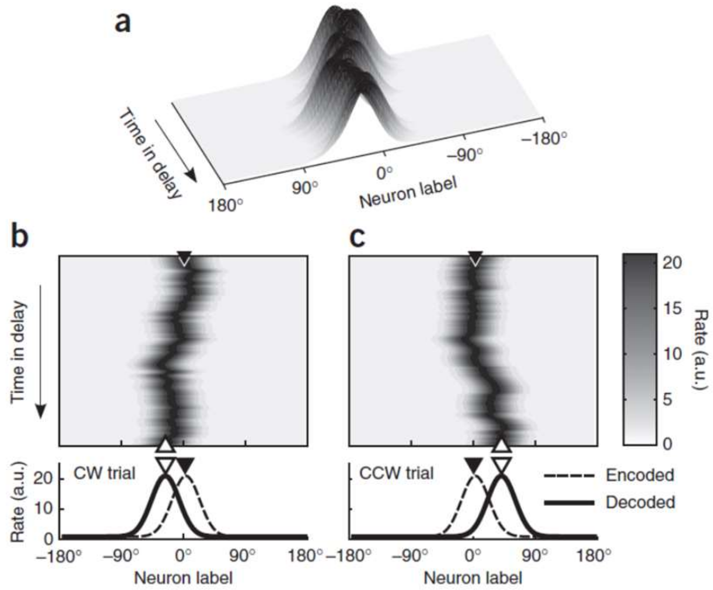

New Mathematical Challenges

- Bump attractor of Amari model insufficient as a neural substrate of a working memory (WM) function.

1. Non-existence of **multi-bump solutions** as model of multi-item memory.
2. Bump shape should depend on **input caracteristics** such as for instance strength and duration to express WM quality.
3. Bump attractor should be robust to **perturbations** of the assumed **symmetry** of the coupling function.

Amari Model with Two Localized Inputs

- Mexican-hat coupling function

  - **Competition**

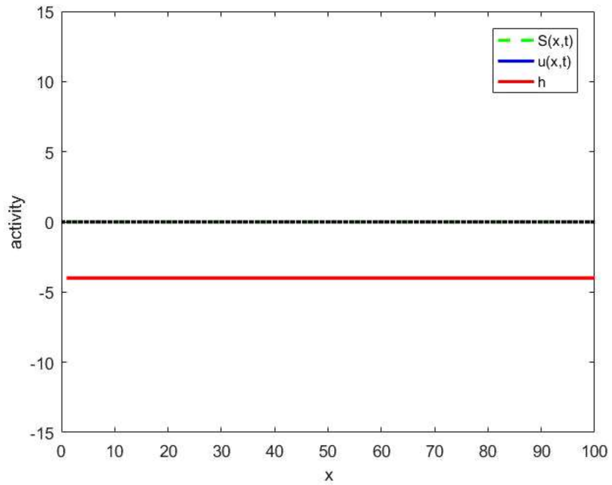

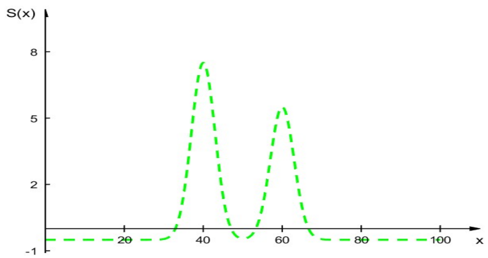

$$S(x) = 8e^{-\frac{(x-45)^2}{18}} + 6e^{-\frac{(x-60)^2}{18}} - 0.5$$

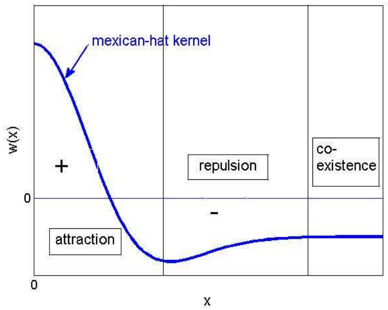

  - **Distance-dependent interaction effects**

Attraction

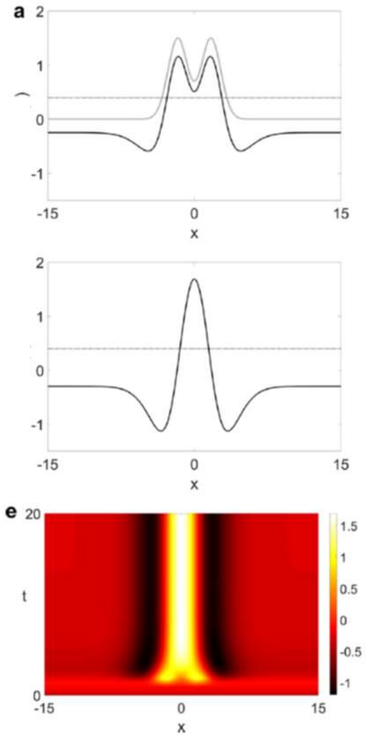

Repulsion

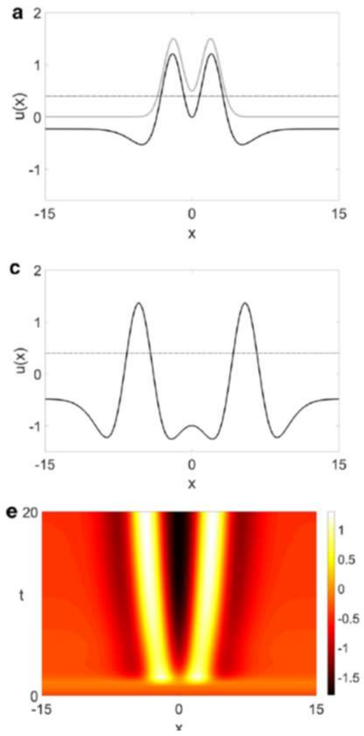

1. Challenge: Oscillatory Coupling Function

(H1) $w(x)$ is symmetric, i.e., $w(-x) = w(x)$ for all x ∈ R
(H2) $w(x)$ is both continuous and integrable on R
(H3) $w(x)$ is an oscillatory function that tends to zero as x→ $\pm\infty$
(H4) $w(0) > 0$ and $w(x)$ has infinite positive zeros at values $z_n, n\epsilon N$

$$w(x) = A\, e^{-k|t|}(k \sin|\alpha x| + \cos|\alpha x|) \text{ with } A > 0 \text{ and } k < \alpha \leq 1$$

The coupling function has zeros given by:

$$z_n = -\frac{\arctan\left(\frac{1}{k}\right) + n\pi}{\alpha} \quad \forall n \in N$$

Laing et al, *SIAM J. Appl. Math*. (2002)
Ferreira et al*, PhysicaD* (2016)

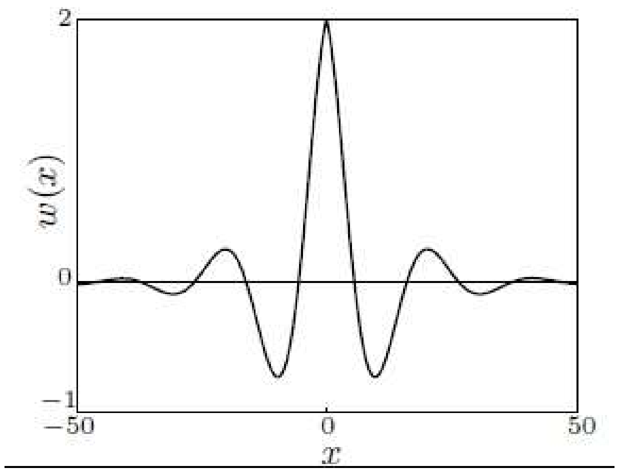

Existence and Stability of a Two-bump Solution

(Fereira et al, *PhysicaD*, 2016)

Theorem: Assume that for an oscillatory coupling function $w(x)$ statisfying (H1)-(H4) the following hypothesis holds:

$$W(z_2) > \frac{p_1 p_2}{\left(1 + e^{\frac{2k\pi}{\alpha}}\right)}, \text{with } p_1 = \frac{A}{k^2 + \alpha^2}, p_2 = \alpha k + k.$$

If $a = \frac{\pi}{\alpha}$ and $b \epsilon (z_2, z_3)$ such that $W(b) = p_1 p_2$, then

$$u(x) = W\left(x + \frac{b+a}{2}\right) - W\left(x + \frac{b-a}{2}\right) + W\left(x - \frac{b-a}{2}\right) - W\left(x - \frac{b+a}{2}\right) - \mathrm{W}\left(\frac{\pi}{\alpha}\right)$$

defines a stable two-bump solution with $R[u] = \left(-\frac{b+a}{2}, -\frac{b-a}{2}\right) \cup \left(\frac{b-a}{2}, \frac{b+a}{2}\right)$.

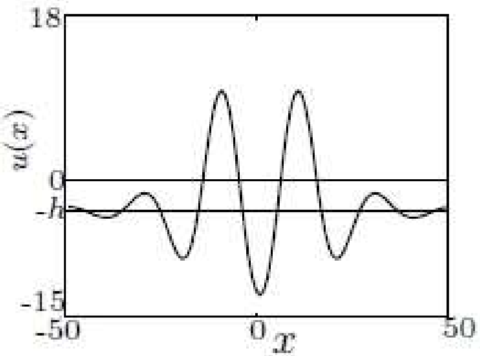

Input-driven Two-Bump Solutions

External input $S2(x,t)$ of bimodal shape centered at $x = 0$ statisfies:

(SH1) $S2(x)$ is continuous on R and symmetric in relation to the center.
(SH2) $S2(x) > 0$ on $(\bar{x}_1, \bar{x}_2), S2(x) < 0$ on $(0, \bar{x}_1) \cup (\bar{x}_2, \infty)$ and $S2(\bar{x}_1) = S2(\bar{x}_2) = 0$.
(SH3) $S2(x)$ is increasing on $\left(0, \frac{\bar{x}_2 - \bar{x}_1}{2}\right)$, and is decreasing on $\left(\frac{\bar{x}_2 - \bar{x}_1}{2}, \infty\right)$.

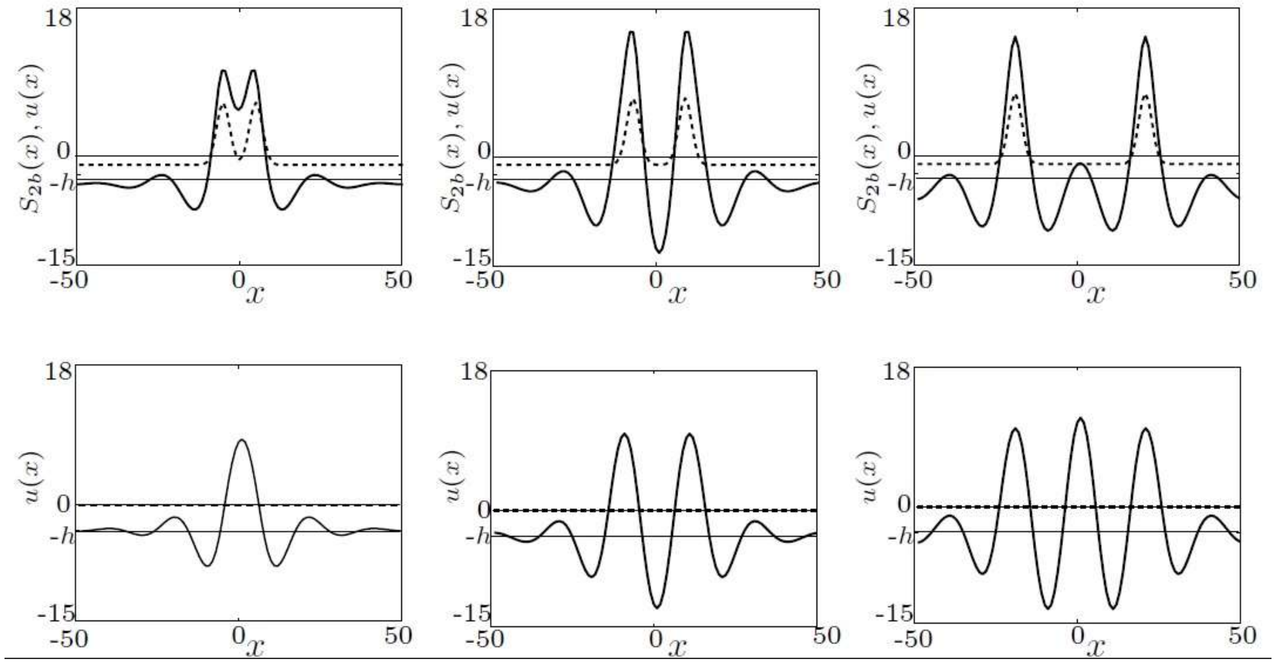

"ON"

"OFF"

Input-driven Two-bump Solutions

- Additional conditions on input shape necessary to guarantee that the solution with $S2(x) > 0$ is in the basin of attraction of the two-bump solution when the input is removed:

$$S2\left(\frac{\bar{x}_2 - \bar{x}_1}{2}\right) > W\left(\frac{\pi}{\alpha}\right),\ \ S2\left(\frac{z_1}{2}\right) < 0,\ \ S2\left(\frac{z_2}{2}\right) > 0,\ S2\left(\frac{z_3}{2}\right) > 0$$

and $S2\left(\frac{z_4}{2}\right) < 0$

(Theorem 6, Ferreira et al. 2016)

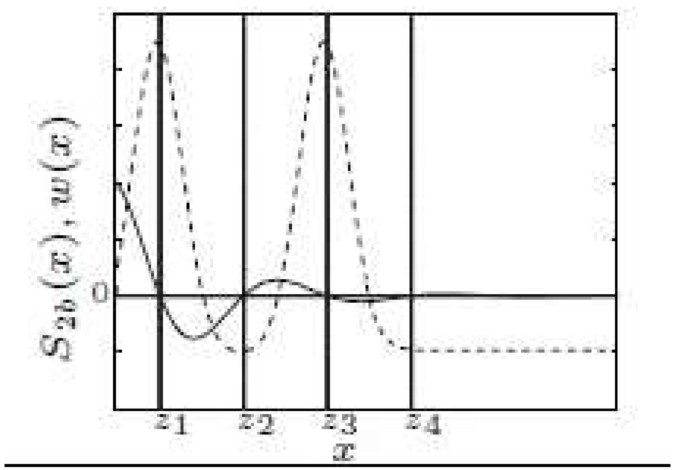

Input-driven Two-bump Solution

- oscillatory coupling function

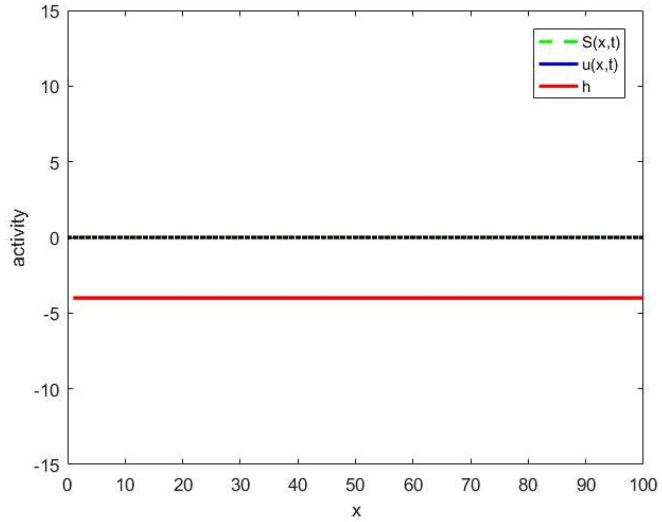

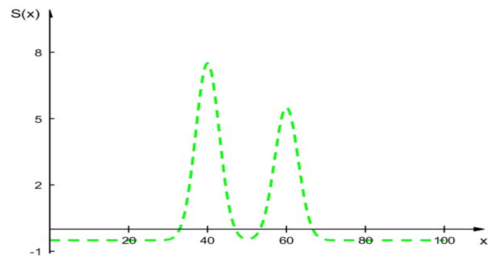

$$S(x) = 8e^{-\frac{(x-45)^2}{18}} + 6e^{-\frac{(x-60)^2}{18}} - 0.5$$

Input-driven Multi-bump Solutions

$w(x) = A\, e^{-k|t|}(k \sin|\alpha x| + \cos|\alpha x|)$ with $A > 0$ and $k < \alpha \leq 1$

Input **on** $S(x) \neq 0$

2nd Input   4th Input   5th Input

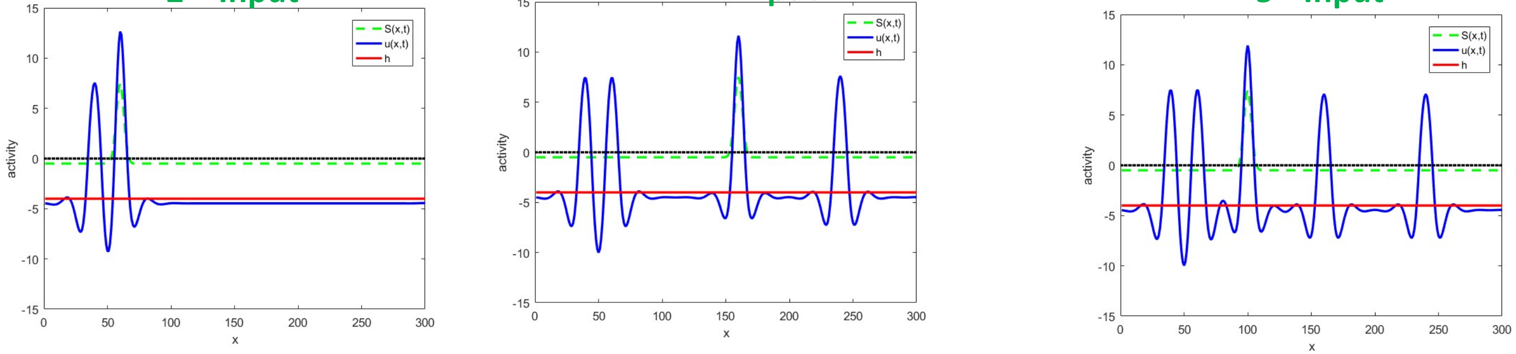

Input **off** $S(x) = 0$

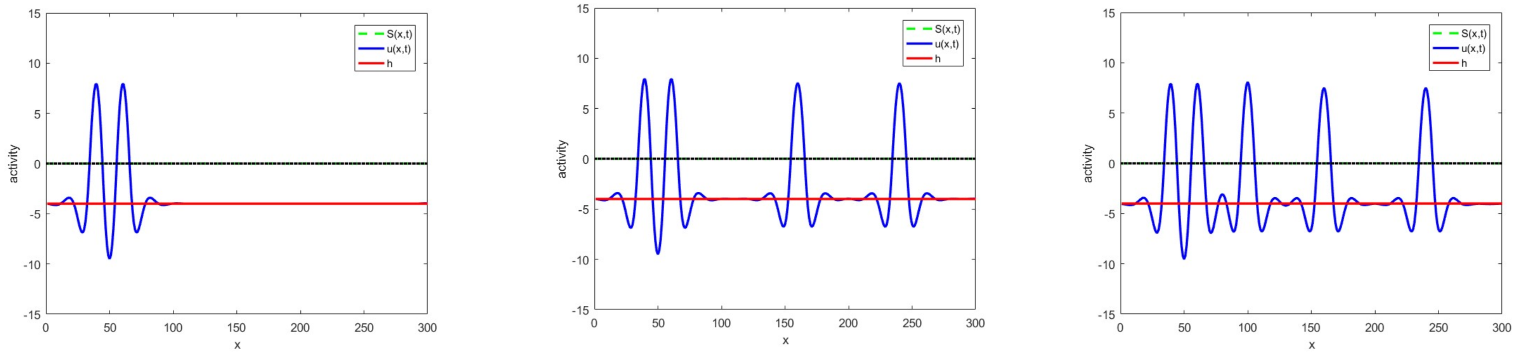

2. Challenge: Novel Two-field Model

- bump shape should reflect input characteristics beyond position
- model of a robust neural integrator of external inputs

Wojtak et al., *Biol. Cybern.* (2021)
Wojtak et al., *NCA* (2021)

$$\frac{\partial u(x,t)}{\partial t} = -u(x,t) + \boldsymbol{v(x,t)} + \int_{-\infty}^{+\infty} w(|x-y|)f(u(y,t) - \Theta)dy + S(x,t)$$

$$\frac{\partial v(x,t)}{\partial t} = -v(x,t) + \boldsymbol{u(x,t)} - \int_{-\infty}^{+\infty} w(|x-y|)\, f(u(y,t) - \Theta)dy$$

- θ = threshold
- w = Mexican-hat or oscillatory connectivity function

Bumps with Input Characteristics

- **two-dimensional continuous attractor**: position and amplitude

Input strength

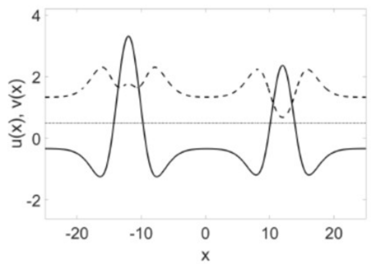

Input width

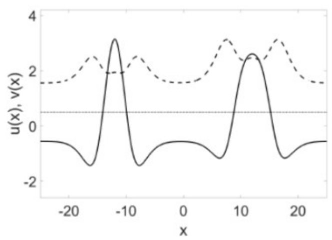

Continuously increasing input strength

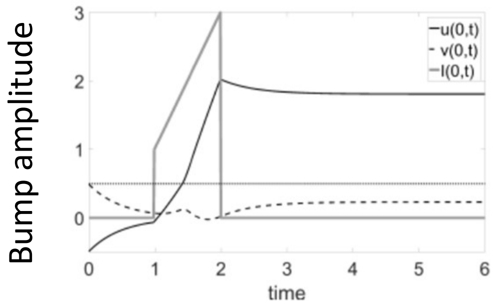

Two sequential inputs

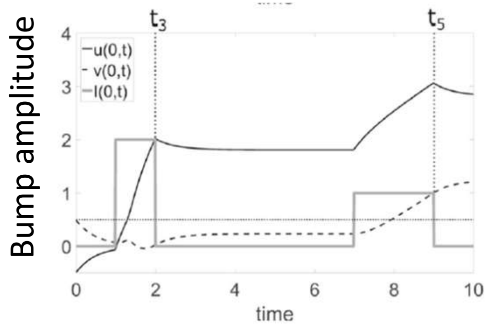

Measuring and Reproducing Time Intervals

M. Jazayeri and M. Shadlen , Curr. Biol., 2015
Recordings in Lateral Intraparietal Cortex (LIP)

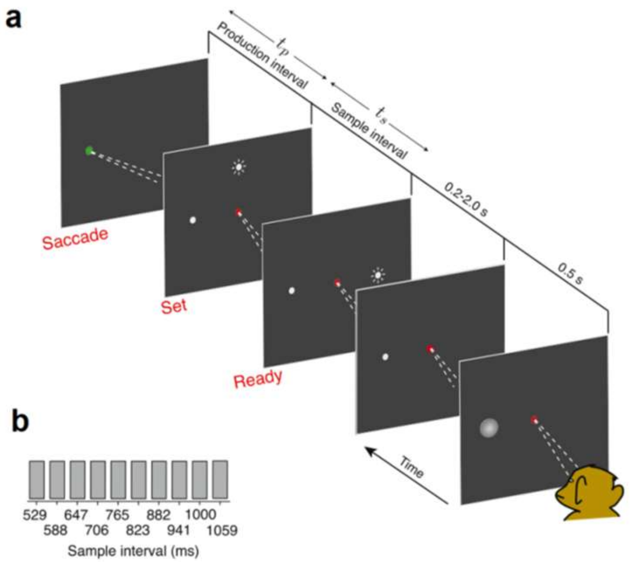

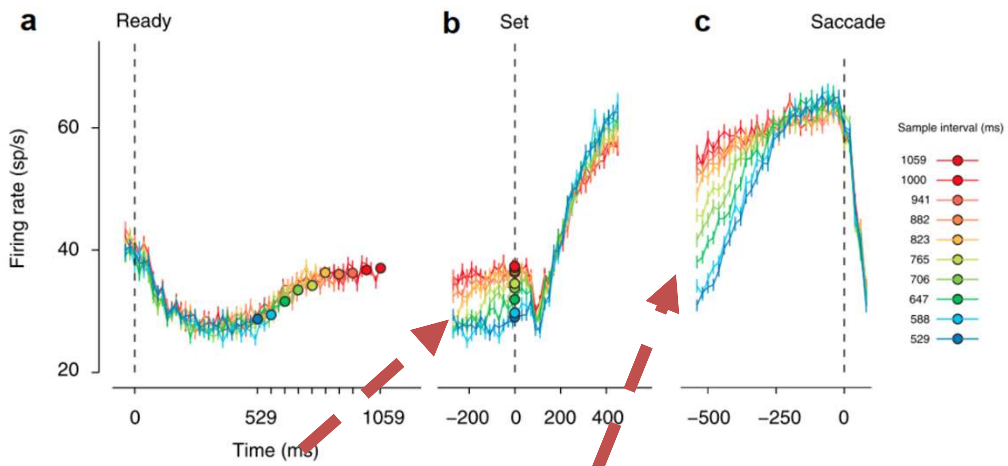

- activity level u_{max} at end of **measurment** reflects elapsed time
- build-up rate of ramping activity during **production** is inversely proportional to u_{max}

Two-Field Neural Integrator

- Mesurement

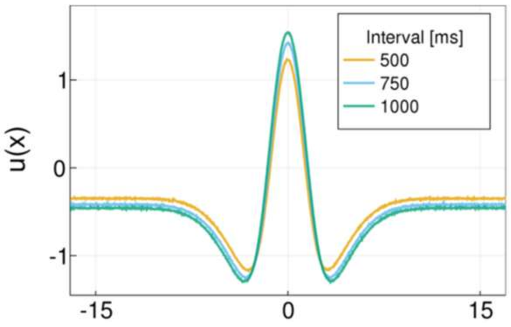

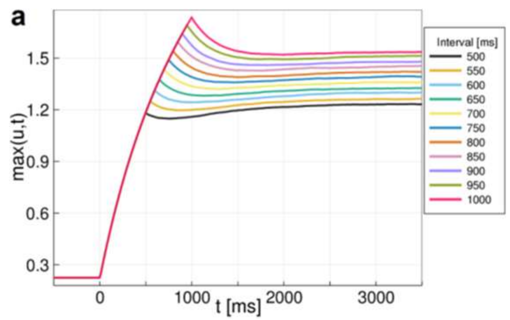

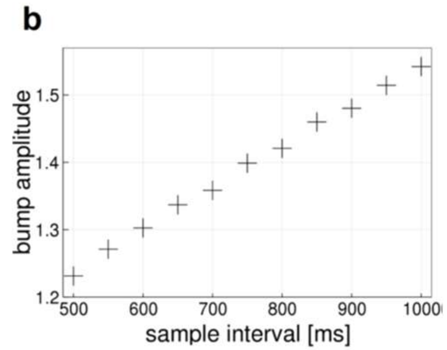

- Production

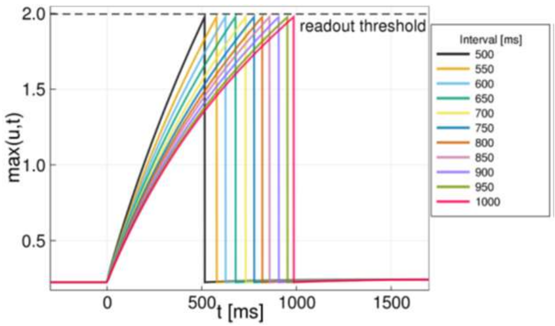

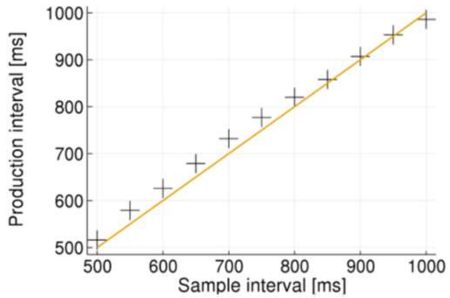

Wojtak et al, ICDL (2019)

Analysis of Bump Solutions

- Analytical techniques used for the Amari equation

- initial condition $u(x,0)+v(x,0)=k>0$
- derive ODE describing the change of lenght of the excited region $\Delta(t)=x_2(t)-x_1(t)$

$$\frac{d\Delta}{dt}=\left(\frac{1}{c_1}+\frac{1}{c_2}\right)(-2\Theta+k+W(\Delta)) \quad \text{with } c_1=\frac{\partial u(x_1,t)}{\partial x},\ -c_2=\frac{\partial u(x_2,t)}{\partial x}$$

- existence of bump solutions of width $\Delta = x_2 - x_1$ determined by the roots of

$$F(\Delta) = -2\,\Theta + k + W(\Delta) = 0$$

- a bump of width Δ is stable if $\frac{dF(\Delta)}{d\Delta} < 0$ holds and unstable otherwise.

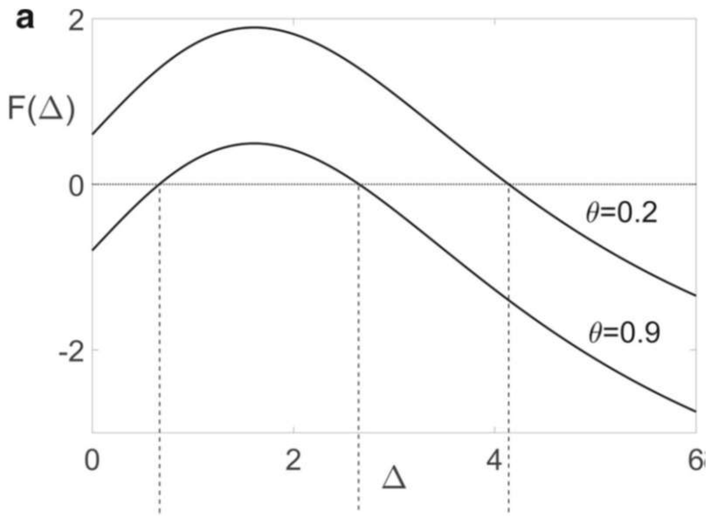

Analysis of Bump Solutions

➢ **Numerical continuation** technique to track solutions as model parameters change

Bifurcation curves with threshold Θ *as* **continuation parameter**

- example solutions at points P_1, P_3 (stable) and P_2 (unstable).

Different input strenghts

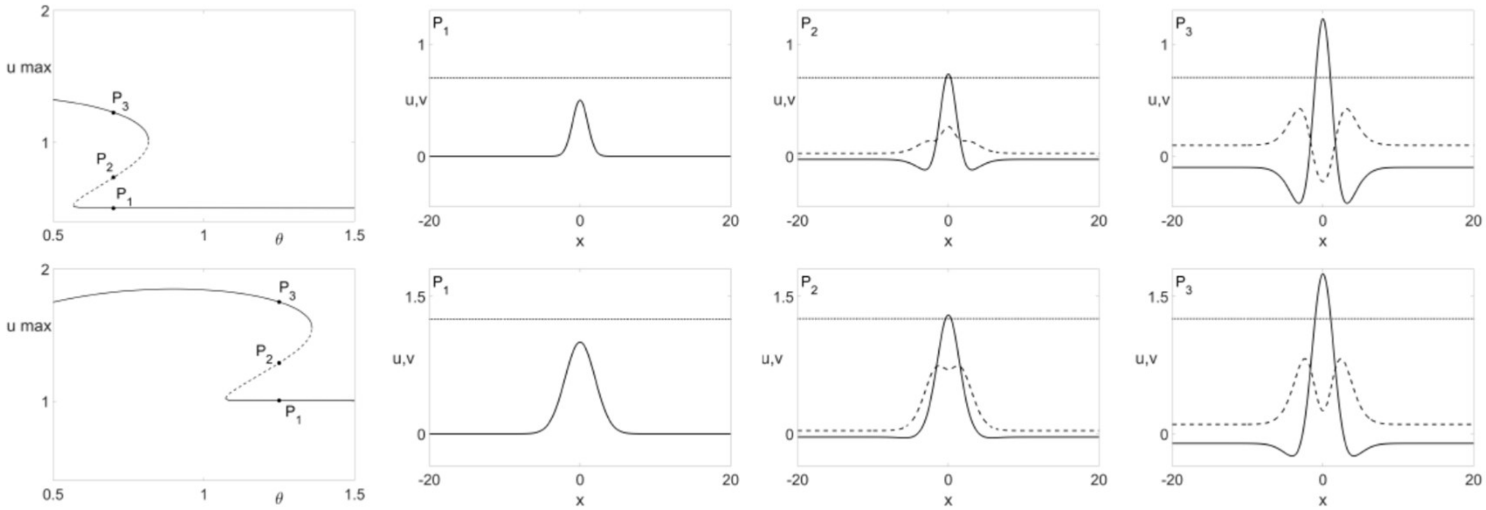

Analysis of Bump Solutions
Two-dimensional case: $r \in \Omega \subset \mathbb{R}^2$

Wojtak et al., *Cog. Neurodynamics (in press)*

$$\frac{\partial u(\boldsymbol{r},t)}{\partial t} = -u(\boldsymbol{r},t) + v(\boldsymbol{r},t) + \int_\Omega w(|\boldsymbol{r}-\boldsymbol{r}'|)f(u(\boldsymbol{r}',t)-\Theta)\boldsymbol{dr}' + S(\boldsymbol{r},t)$$

$$\frac{\partial v(\boldsymbol{r},t)}{\partial t} = -v(\boldsymbol{r},t) + u(\boldsymbol{r},t) - \int_\Omega w(|\boldsymbol{r}-\boldsymbol{r}'|)f(u(\boldsymbol{r}',t)-\Theta)\boldsymbol{dr}'$$

Radially symmetric bump solutions (with radius R)

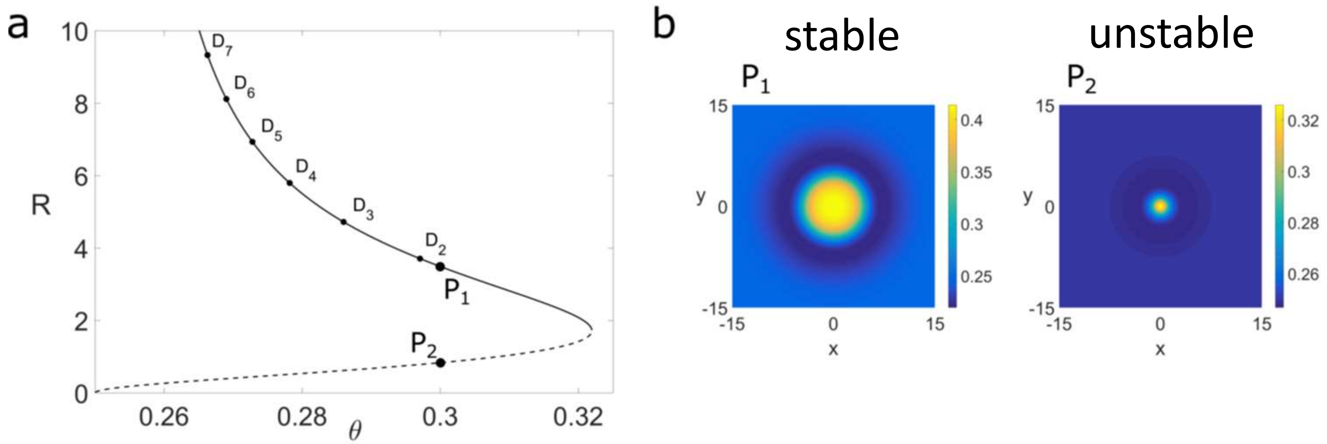

Difference to 1D Model

- Low-order perturbations of a radially symmetric 2D bump exhibiting D_n symmetry

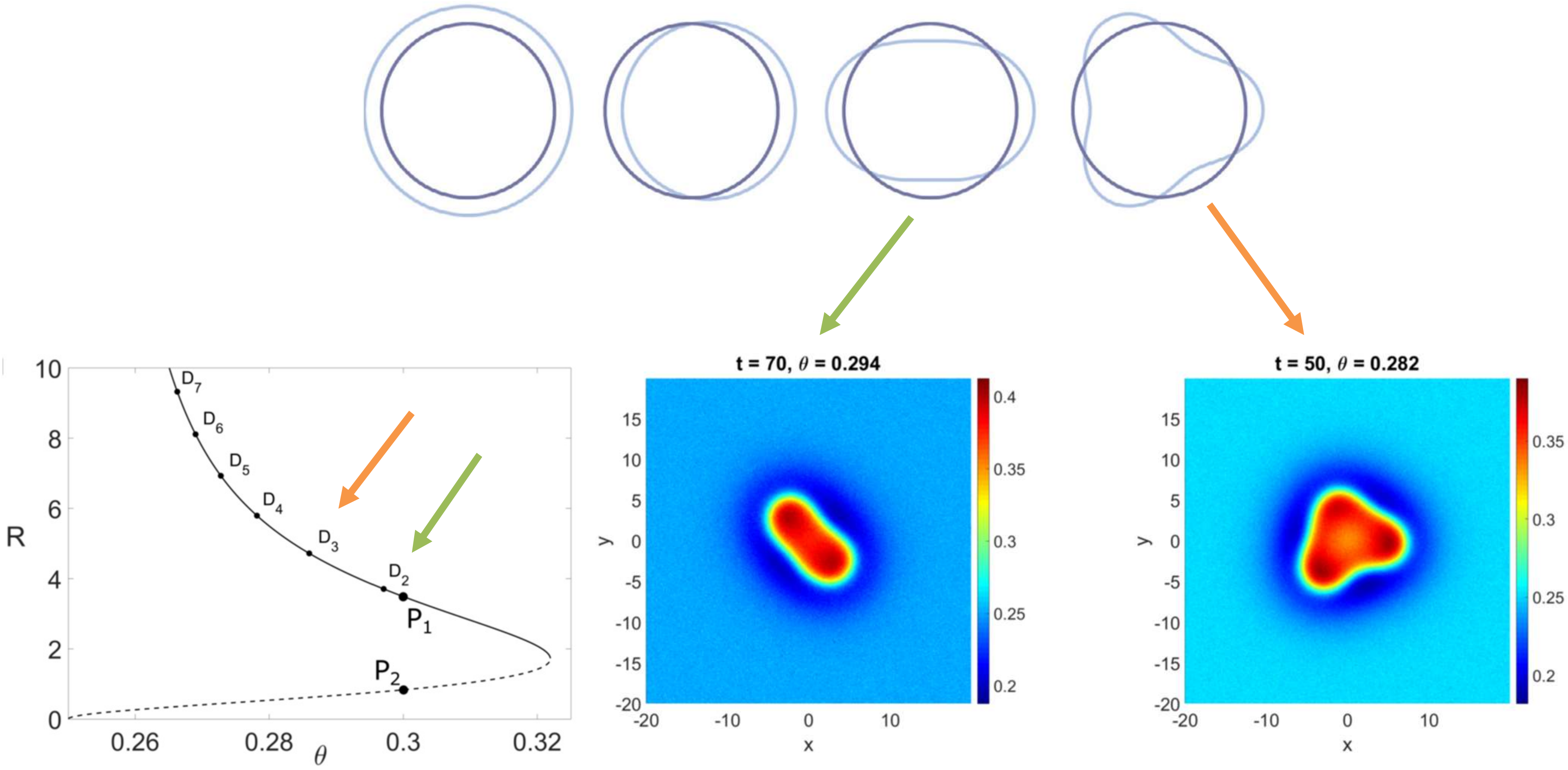

Numerical Continuation

- determine range of parameter values supporting a bump solution

Bifurcation curves for threshold parameter Θ of the 2D model

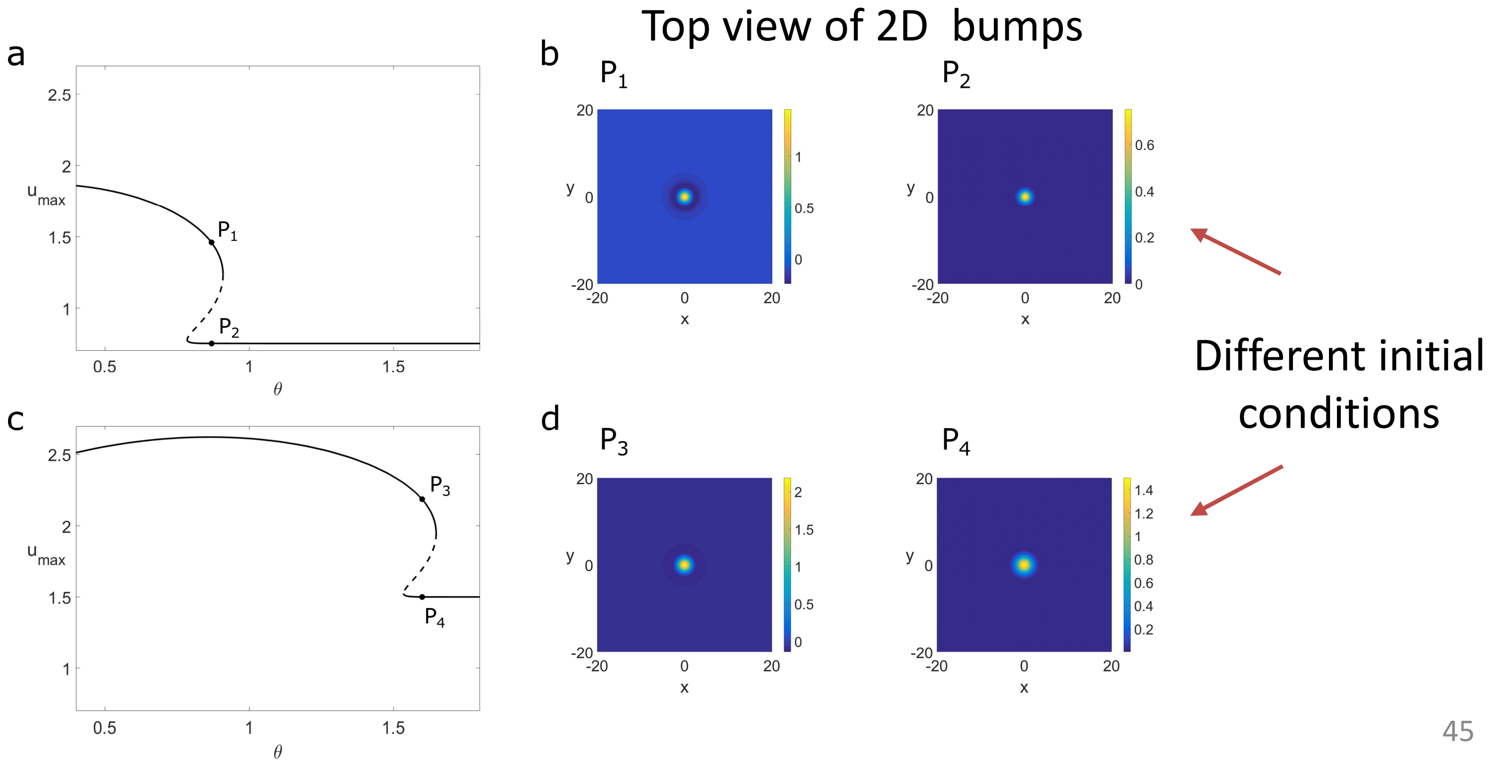

3. Challenge: Structural Stability of Bump Formation

- Any perturbation of the assumed **perfect symmetry** of the interaction kernel distroys the continuous bump attractor of the **Amari model**

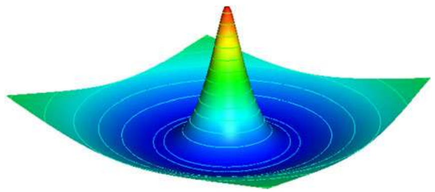

<u>Example:</u> **2D Mexican-hat** kernel with noise

(a,b) Cross sections of kernel

(c) Bump drift in a single trial

(d) Trajectories of bump centroid over 100 trials, starting at ***r**=(0,0)*

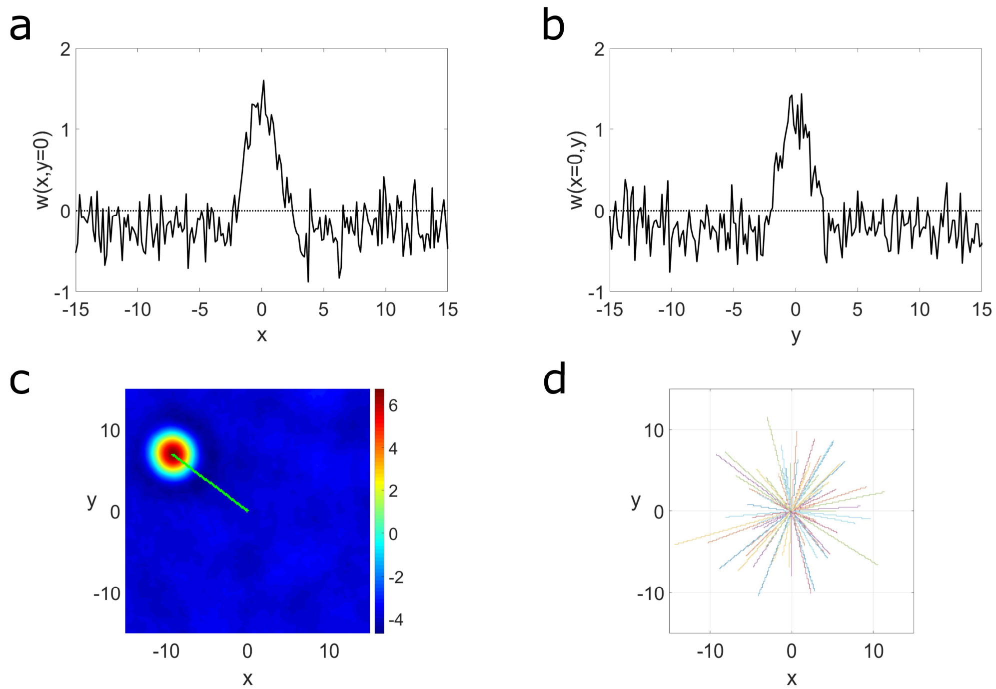

Structual Stability of Bump Formation

- The novel **two-field model** does not require the biologically unrealistic symmetry assumption
  $\Longrightarrow$ Model of robust working memory

<u>Example:</u> **2D Mexican-hat** kernel with noise

(e) Stationary 2D bump at $\boldsymbol{r}$*=(0,0)*

(f) Trajectories of bump centroid over 100 trials, starting at $\boldsymbol{r}$*=(0,0)*

(g,h) Cross sections of 2D bump

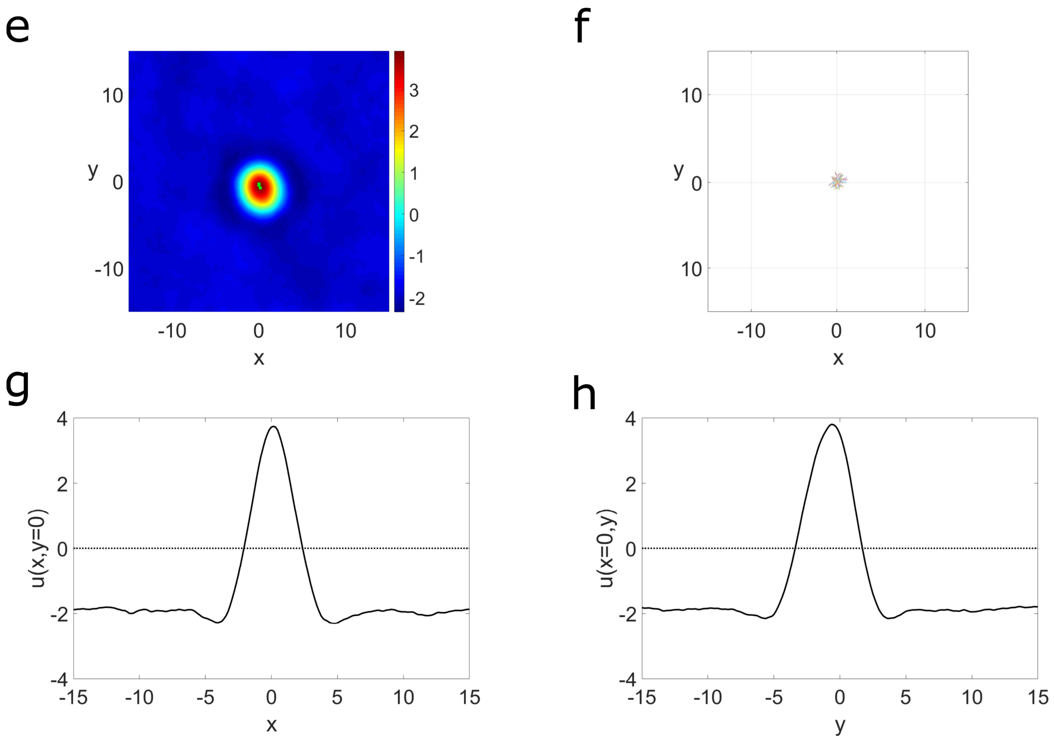

Quasicrystal Patterns

Amari model

with $\beta = 0.39$,
$\theta = 2.371$,
$b_1 = 0.691$,
$b_2 = 0.619106$,
$\alpha_1 = 2.144141$,
$\alpha_2 = 0.518136$,
$s_1 = 0.574835$,
$s_2 = 0.236861$
and $q = 2\cos(\pi/5)$.

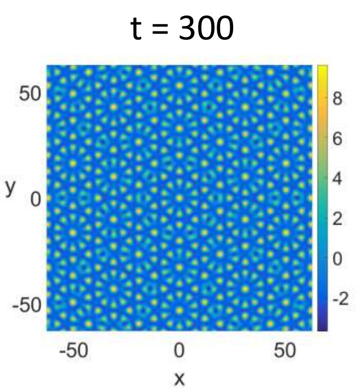

The kernel w is given by:

$$w(r) = \alpha_1 p(r,b_1,s_1,1) + \alpha_2 p(r,b_2, s_2,q),$$

where

$$p(r,b,s,q) = \exp(-sr)[\cos(qr)+b \sin(qr)]$$

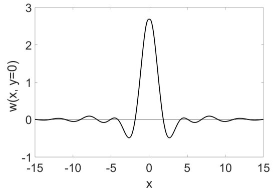

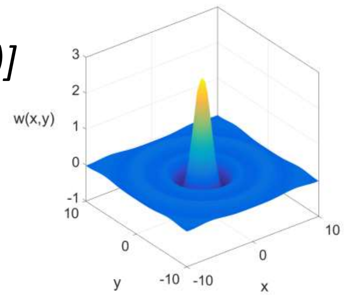

Two-field model

with $\beta = 1$, $\theta = 3$, $b_1 = 0.7$, $b_2 = 0.6$,
$\alpha_1 = 2.15$, $\alpha_2 = 0.5$, $s_1 = 0.6$, $s_2 = 0.25$ and
$q = 2\cos(\pi/5)$.

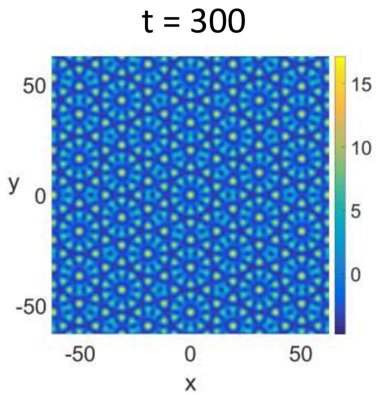

Numerical continuation result

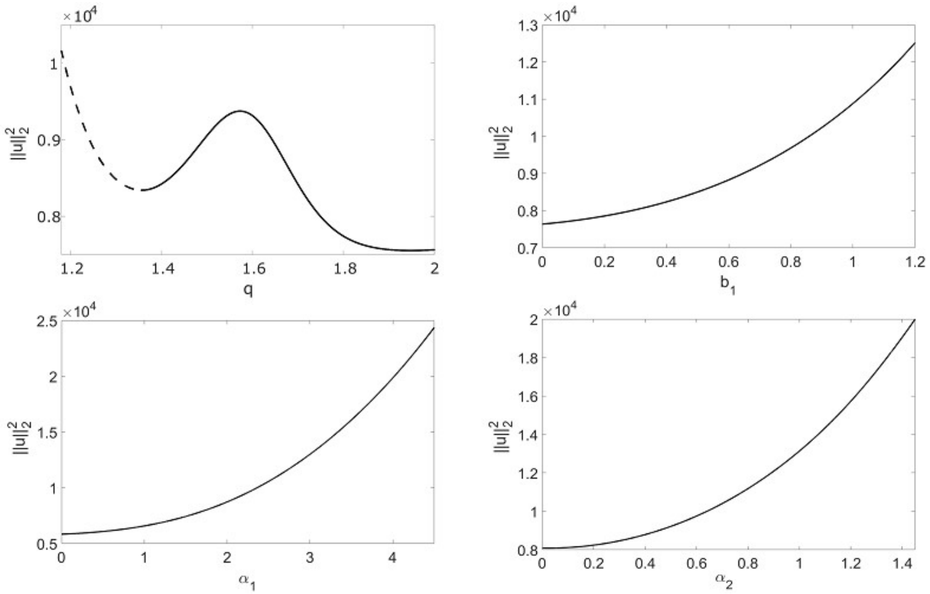

Application for Cognitive Artifical Agents

Case study: Sequence learning

Many of our everyday activities involve the production of ordered sequences of basic actions:

- preparing a cup of tea,
- assemble a piece of furniture from its components,
- playing a melody,
- daily traveling routine.

Learning Serial Order: Different Theories

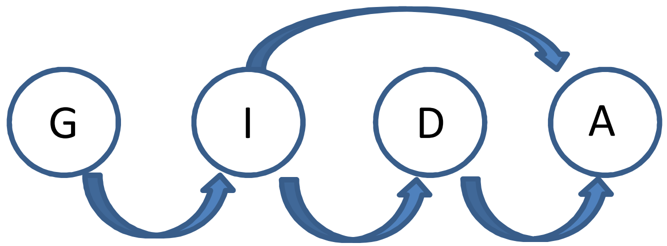

Chaining theory

e.g., Wickelgreen (1969)

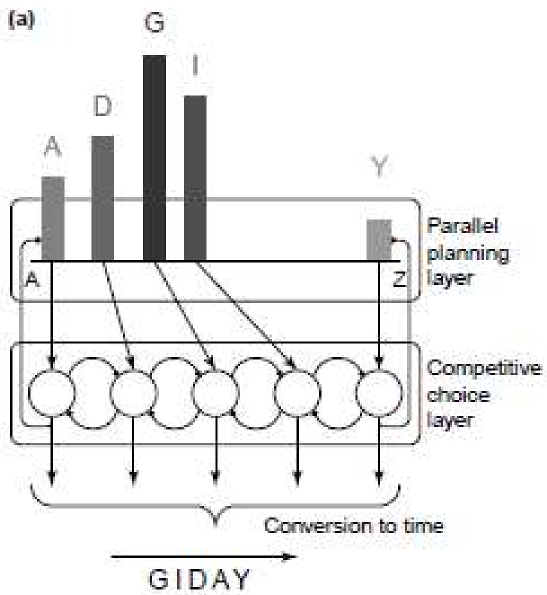

Ordinal theory

e.g., Bullock (2001)

Ordinal Theory: Neurophysiological Evidence

- Monkeys draw geometrical shapes from a screen
- Parallel activation of all movement segments:
  - strenght of pre-activation of neural populations in prefrontal cortex reflects the rank order of movement segments.

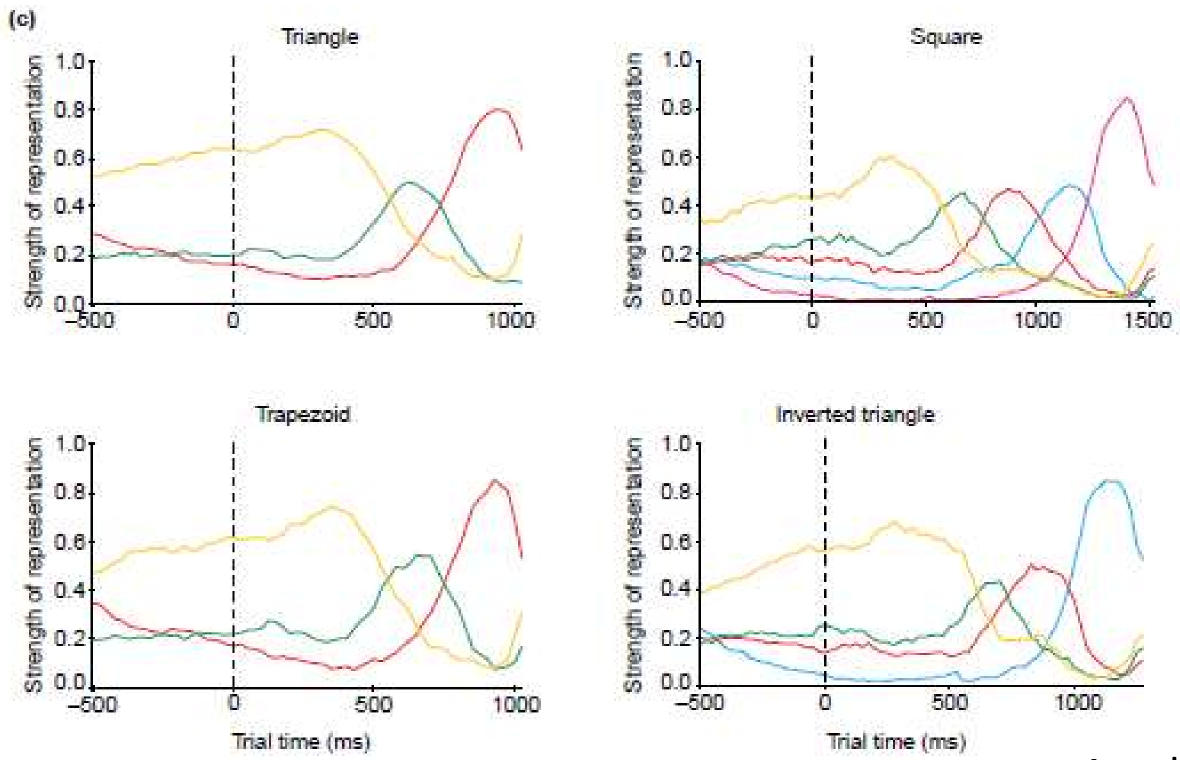

Averbeck et al., *PNAS* (2002)

Sequence Learning

Example: Serial order of manipulating **colored** objects

- Stable **multi-bump pattern** as multi-item memory

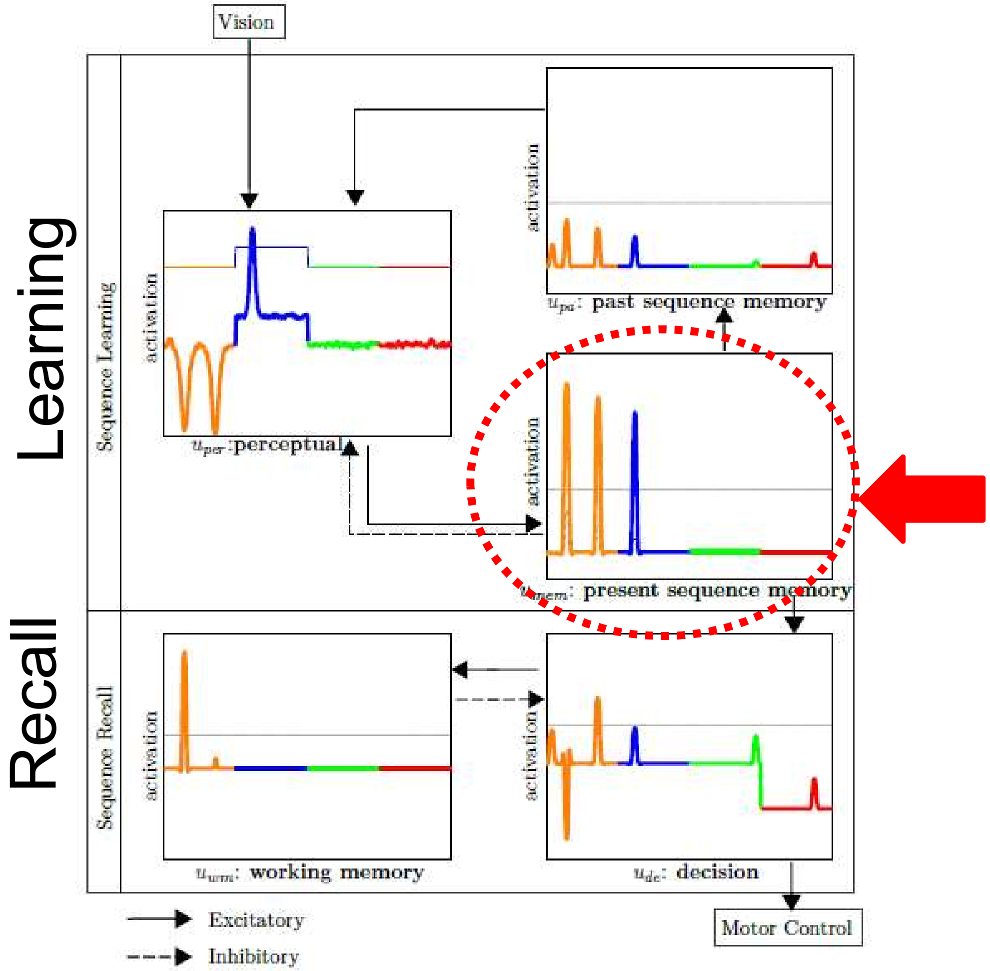

Stable activation gradient represents memory of serial order and relative timing of events.

Ferreira et al., *TCDS* (2021)

Model Equations

Example: Perceptual Field u_{per}

$$\tau \frac{\partial u_{per}(x,t)}{\partial t} = -u_{per}(x,t) + \int w_{lat}(x - x')f(u_{per}(x',t))dx' +$$

$$+u_{MT}(x,t) \qquad + \qquad I(x,t) \qquad + \qquad \zeta(x,t)$$

excitatory input Memory Trace — external input — noise

$$-\int w_{osc}\ (x - x')f(u_{M_{on}}(x',t)dx$$

inhibitory feedback from Memory Field

Learning

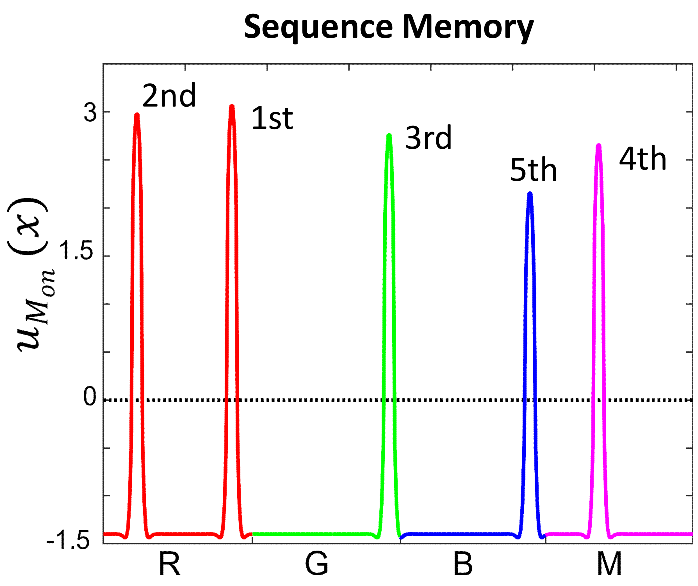

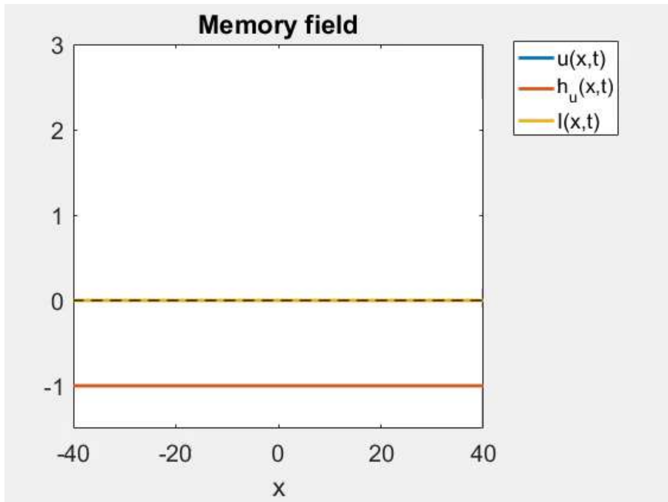

Activation gradient is established by a state-dependent resting level dynamics:

$$\frac{\partial h_{M_{on}}(x,t)}{\partial t} = \beta_M f(u_{M_{on}}(x,t)) \int_{\Omega} f(u_{Start}(x))\mathrm{d}x$$
$$+[1 - f(u_{M_{on}}(x,t))][-h_{M_{on}}(x,t) + h_{M_0}]$$

Recall

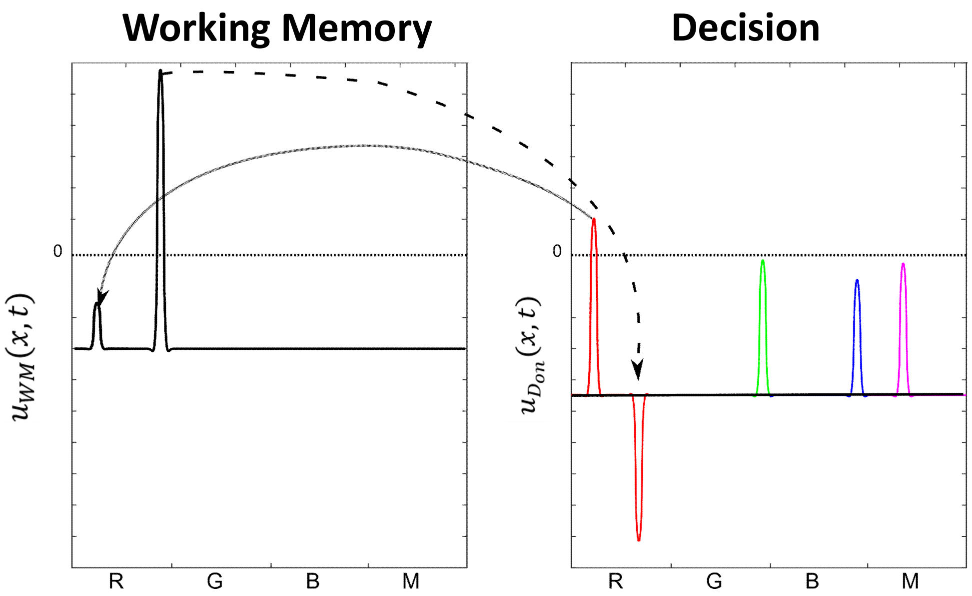

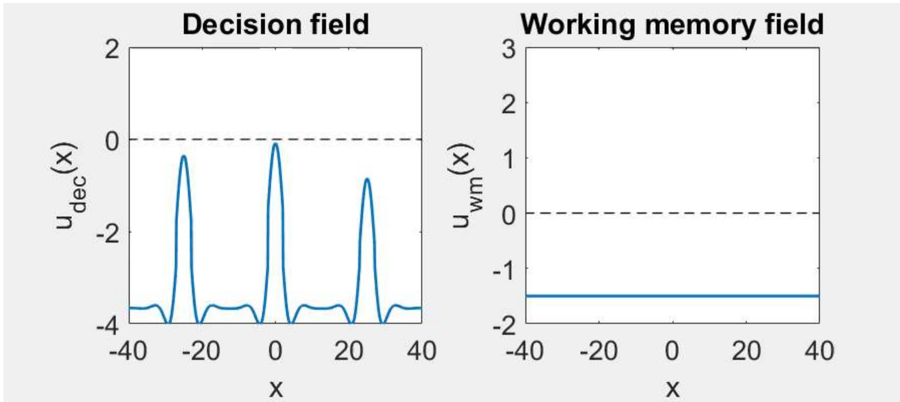

Ramp-to threshold dynamics of the baseline activity in the decision field u_D receiving the activation gradient as subthreshold input:

$$\frac{\mathrm{d}h_D(t)}{\mathrm{d}t} = \beta_D \int_\Omega f(u_{Start}(x))\mathrm{d}x + c_h \epsilon(t)$$

Human-robot Interaction: Pipe Assembly Task

- Robot **Sawyer** learns the sequential order by observering a human team

- During joint task execution, **Sawyer** hands over to the human user the different pipes in the correct order

Wojtak et al., *NCA* (2021)

Task Demonstration

- 2D two-field model: object color and lenght as dimensions

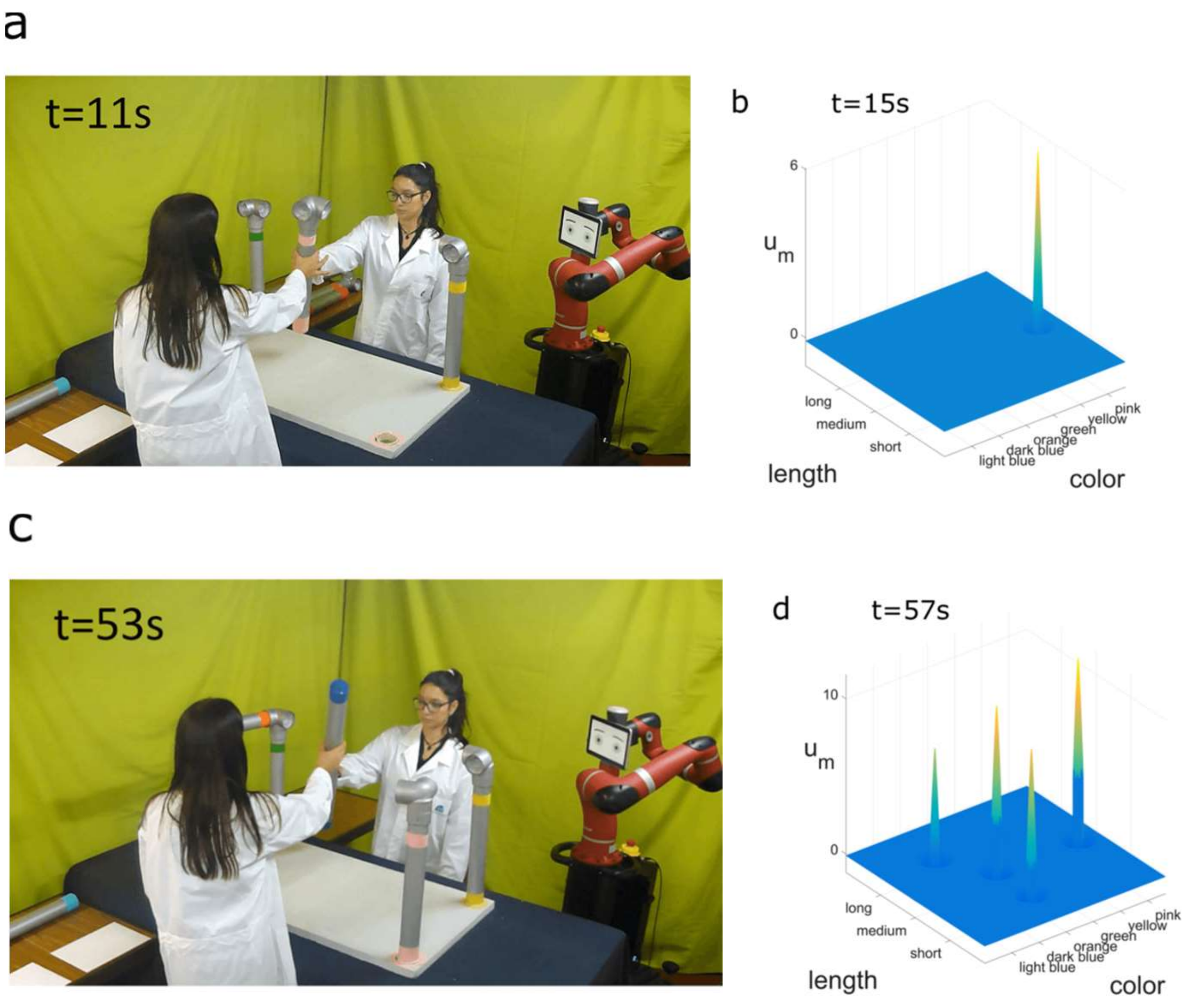

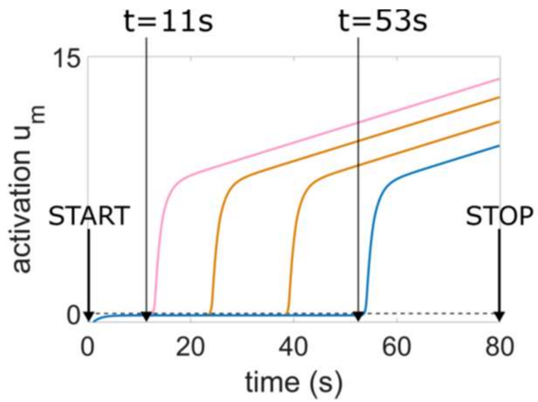

Time course of activity
in the memory field

Joint Task Execution

- Autonomous recall of sequential order in the decision field

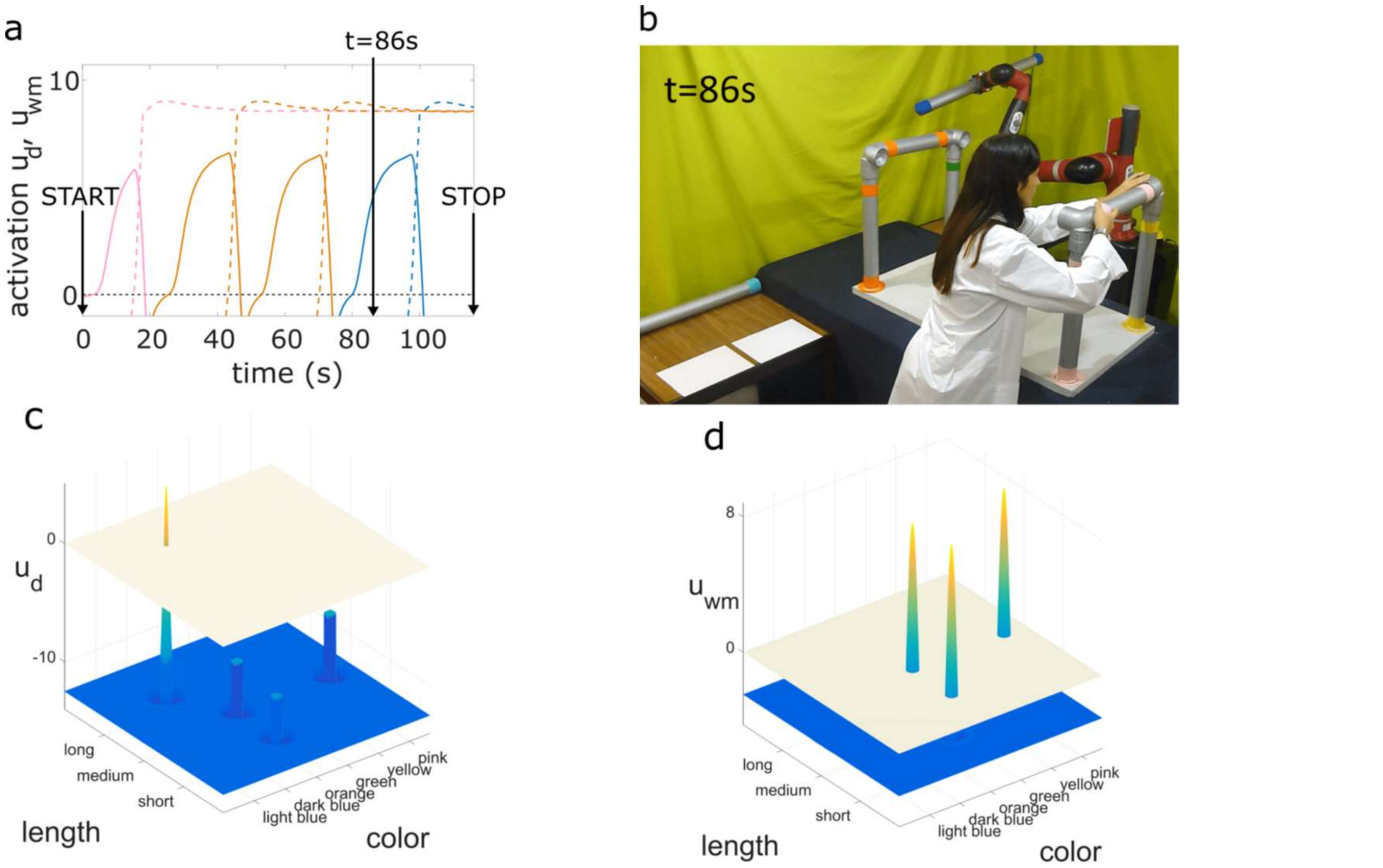

Formation of the first bump in the decision field

Memory of already excuted object transfers

Musical Sequence

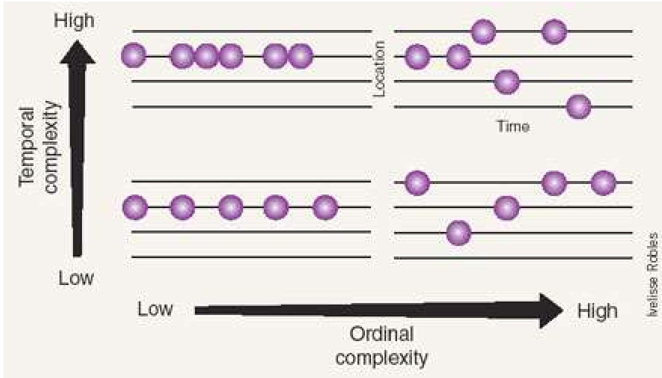

- Challenging example for sequence learning models
  - integration of order and timing
  - events often repeat in different contexts

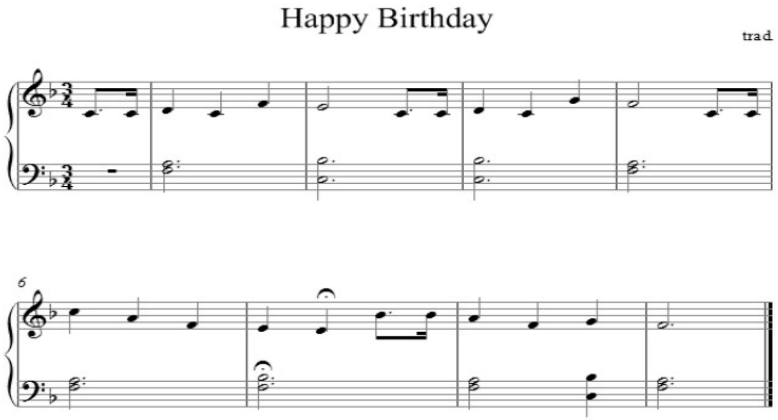

- Despite its complexity, music is highly memorable!

Experiment with Humanoid Robot *ARoS*

- Teacher demonstrates the "Happy Birthday" sequence and ARoS has to perfom the sequence from memory.
- Simplifications: Learning the "what" and "when" but not the "how".
  - Sequence is colour coded, auditory channel also possible
  - 6 Fingers (2 hands) of ARoS positioned over the keys

Sequence : C - C - D - C - F - E - C - C - D - C - G - F

Mathematics in Action:
Observational Learning of a Musical Sequence

Ferreira et al, IEEE TRANSACTIONS ON COGNITIVE AND DEVELOPMENTAL SYSTEMS (2021)

Experimental Results

- here only the first 6 events for simplicity

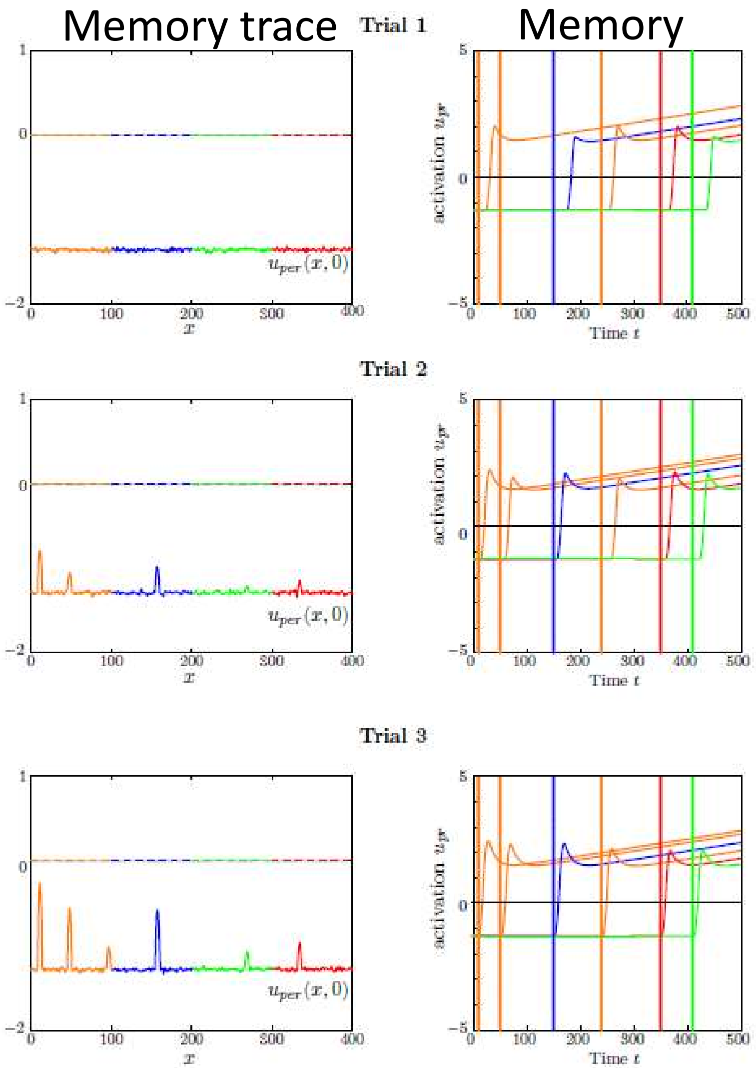

Experimental Results

- different execution speeds: relative timing preserved

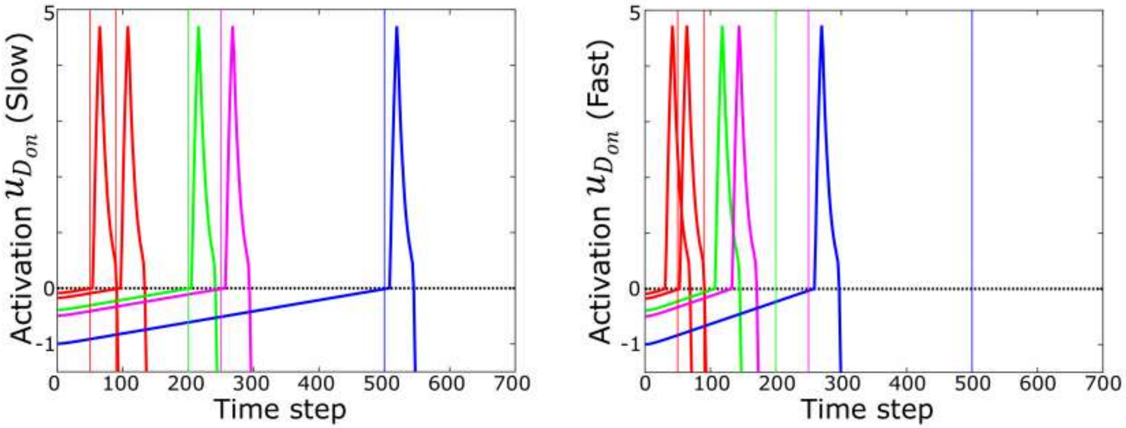

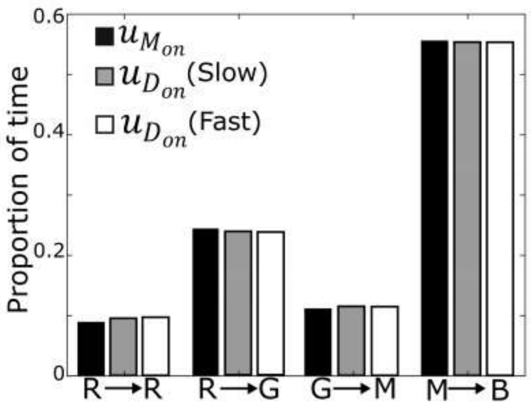

$$\frac{\mathrm{d}h_D(t)}{\mathrm{d}t} = \beta_D \int_\Omega f(u_{Start}(x))\mathrm{d}x + c_h\epsilon(t)$$

$$\boxed{\beta_D(Slow) < \beta_D(Fast)}$$

Learning Driver Routines

- develop a cognitive system capable of learning and predicting the habits and preferences of the occupants of a vehicle from GPS data:
  - Where to go?
  - When to go?
  - How long to stay there?
  - Who the next driver(s)/passenger(s) is(are)?
  - Which objects come in(out)?

BOSCH

"Easy Ride:Experience is everything"

Learning Driver Routines

- fields spanned over the GPS coordinates *Longitude* and *Latitude*

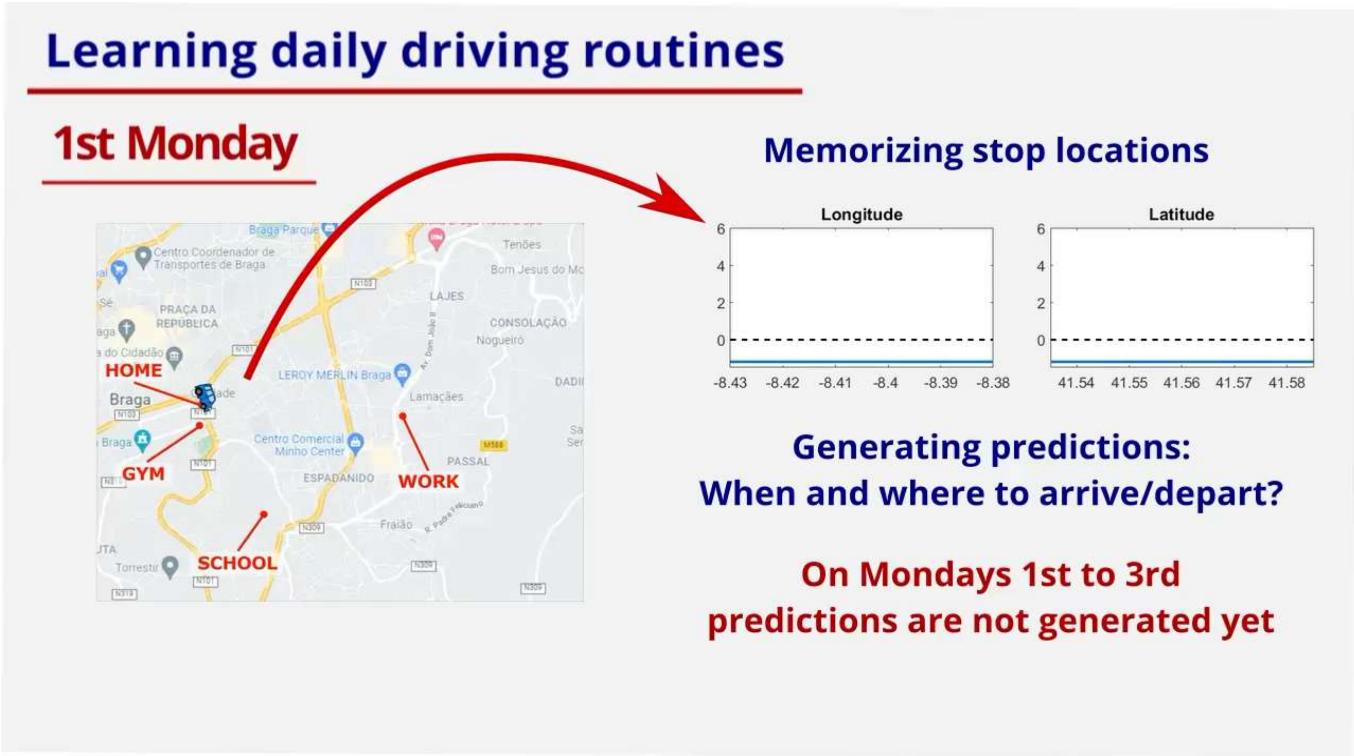

Predicting Driver Routines

- routine event: visted in two consecutive weeks
- time window for recall: anticipation + tolerance

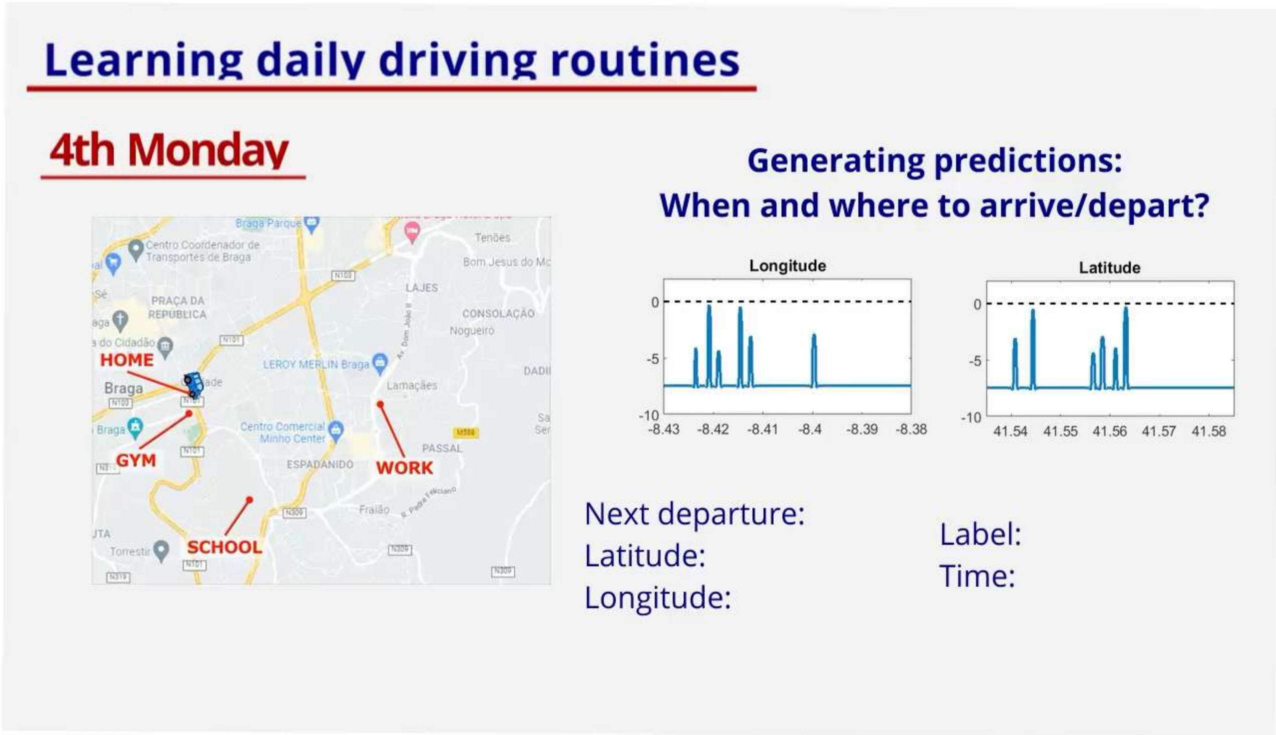

Results

- Real and predicted times in minutes of two different day routines from two different drivers
- GPS data recorded over 11 weeks in the city of Braga

Monday routine of driver A (11 weeks)					Friday routine of driver B (8 weeks)				
Stops	NS	Real time	NP	Predicted time	Stops	NS	Real time	NP	Predicted time
S_1	11	526.5 (±1.81)	9	525.8 (±1.97)	S_1	8	520.0 (±4.11)	6	518.3 (±5.16)
S_2	7	542.1 (±2.19)	9	541.1 (±2.66)	S_2	8	539.5 (±5.88)	6	537.0 (±6.95)
S_3	11	550.1 (±6.45)	9	549.2 (±7.18)	S_3	8	1116.3 (±8.40)	6	1117.0 (±9.67)
S_4	11	1113.1 (±2.07)	9	1112.8 (±2.87)	S_4	3	1132.0 (±3.61)	3	1133.4 (±3.64)
S_5	2	1129.5 (±12.02)	0	–	S_5	8	1261.6 (±5.21)	6	1262.5 (±5.48)
S_6	11	1134.0 (±7.35)	9	1134.0 (±7.67)	–				

NS: number of weeks that the location was **visited**
NP: number of weeks that the location was **predicted**

Wojtak et al., ICCSA (2021)

Conclusions/Outlook

Mathematics of **Dynamic Neural Fields**

Analytical and numerical techniques as complementary tools

New theoretical challenges

- **Learning** a continuous attractor
- Relation to **Deep Learning Neural Network**

  ⇒ learning from big data vs. continual learning

Neuroscience and **Robotics** represent highly interesting application domains for mathematicians

New challenges for **DNF models**

- DNF approach to human-robot interactions
- Multi-target tracking
- Numerosity perception
- Learning driver routines based on GPS data

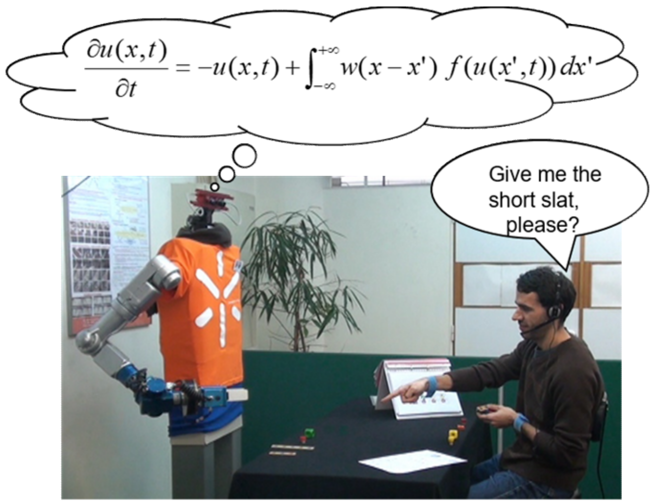

Robot Intelligence?

JAST Project

University of Minho, Portugal

Dept. of Industrial Electronics & Dept. Mathematics for Science and Technology

&

Radboud University Nijmegen, The Netherlands

Donders Institute For Brain, Cognition and Behaviour, Centre For Cognition

User-Evaluation Study

Goal Inference & Conflict/Error Monitoring

European Commission

NETT NEURAL ENGINEERING TRANSFORMATIVE TECHNOLOGIES

CMAT Centro de Matemática

FCT Fundação para a Ciência e a Tecnologia
MINISTÉRIO DA CIÊNCIA, TECNOLOGIA E ENSINO SUPERIOR

- *Estela Bicho*
- *Flora Ferreira*
- *Weronika Wojtak*
- *Paulo Barbosa*
- *Paulo Vincente*
- *Pedro Guimarães*

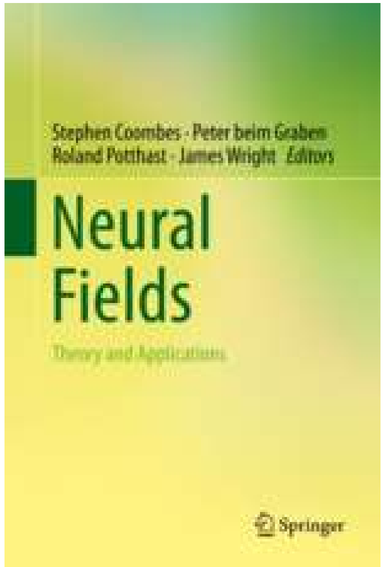

Thank you !

https://github.com/w-wojtak/neural-fields-matlab

Some References

[1] S.-I. Amari (1977). Dynamics of pattern formation in lateral-inhibition type neural fields, *Biological Cybernetics* 27 (2), 77-87.

[2] W. Erlhagen, E. Bicho (2006). The dynamic neural field approach to cognitive robotics, *Journal of Neural Engineering* 3 (3), R36

[3] F. Ferreira., W. Erlhagen, E. Bicho (2016). Multi-bump solutions in a neural field model with external inputs. *Physica D: Nonlinear Phenomena*, 326, 32-51.

[4] W. Wojtak, S. Coombes, D. Avitabile,, E. Bicho, W. Erlhagen, (2021). A dynamic neural field model of continuous input integration. *Biological Cybernetics*, *115*(5), 451-471.

[5] F. Ferreira, W. Wojtak, E. Sousa, L. Louro, E. Bicho, W. Erlhagen, W. (2021). Rapid learning of complex sequences with time constraints: A dynamic neural field model. *IEEE Transactions on Cognitive and Developmental Systems*. *13*(4), 853-864.

[6] Lima, P. M., Erlhagen, W., Kulikova, M. V., & Kulikov, G. Y. (2022). Numerical solution of the stochastic neural field equation with applications to working memory. *Physica A: Statistical Mechanics and its Applications*, *596*, 127166.

[7] Wojtak, W., Ferreira, F., Guimarães, P., Barbosa, P., Monteiro, S., Erlhagen, W., Bicho, E., Towards Endowing Intelligent Cars with the Ability to Learn the Routines of Multiple Drivers: A Dynamic Neural Field Model, Lecture Notes in Computer Science (2021), Vol. 12952 LNCS, 337-349